Measurement of the charge ratio of atmospheric muons with the CMS detector

CMS Collaboration ; Khachatryan, V ; Amsler, C ; De Visscher, S ; Chiochia, V ; et al

Abstract: We present a measurement of the ratio of positive to negative muon fluxes from cosmic ray interactions in the atmosphere, using data collected by the CMS detector both at ground level and in the underground experimental cavern at the CERN LHC. Muons were detected in the momentum range from 5 GeV/c to 1 TeV/c. The surface flux ratio is measured to be 1.2766 ± 0.0032 (stat.) ± 0.0032 (syst.), independent of the muon momentum, below 100 GeV/c. This is the most precise measurement to date. At higher momenta the data are consistent with an increase of the charge ratio, in agreement with cosmic ray shower models and compatible with previous measurements by deep-underground experiments.

DOI: https://doi.org/10.1016/j.physletb.2010.07.033

EUROPEAN ORGANIZATION FOR NUCLEAR RESEARCH (CERN)

CERN-PH-EP-2010-011
2010/05/31

CMS-MUO-10-001

Measurement of the charge ratio of atmospheric muons with the CMS detector

The CMS Collaboration*

Abstract

We present a measurement of the ratio of positive to negative muon fluxes from cosmic ray interactions in the atmosphere, using data collected by the CMS detector both at ground level and in the underground experimental cavern at the CERN LHC. Muons were detected in the momentum range from 5 GeV/c to 1 TeV/c. The surface flux ratio is measured to be $1.2766 \pm 0.0032\,(\text{stat.}) \pm 0.0032\,(\text{syst.})$, independent of the muon momentum, below 100 GeV/c. This is the most precise measurement to date. At higher momenta the data are consistent with an increase of the charge ratio, in agreement with cosmic ray shower models and compatible with previous measurements by deep-underground experiments.

Submitted to Physics Letters B

*See Appendix A for the list of collaboration members

1 Introduction

The muon charge ratio R is defined as the ratio of the number of positive- to negative-charge atmospheric muons arriving at the Earth's surface. These muons arise from showers produced in interactions of high-energy cosmic ray particles with air nuclei in the upper layers of the atmosphere. The magnitude and the momentum dependence of R are determined by the production and interaction cross sections of mesons (mainly pions and kaons), and by their decay lengths. As most cosmic rays and the nuclei with which they interact are positively charged, positive meson production is favoured, hence more positive muons are expected. Previous measurements from various experiments [1–8] showed the muon charge ratio to be constant up to a momentum of about 200 GeV/c, and then to increase at higher momenta, in agreement with the predicted rise in the fraction of muons from kaon decays. Measurements of the charge ratio can be used to constrain hadronic interaction models and to predict better the atmospheric neutrino flux.

The Compact Muon Solenoid (CMS) [9] is one of the detectors installed at the Large Hadron Collider (LHC) [10] at CERN. The main goal of the CMS experiment is to search for signals of new physics in proton-proton collisions at centre-of-mass energies from 7 to 14 TeV [11].

Cosmic rays were used extensively to commission the CMS detector [12, 13]. These data can also be used to perform measurements of physical quantities related to cosmic ray muons. This letter presents a measurement of the muon charge ratio using CMS data collected in two cosmic ray runs in the years 2006 and 2008. More details of the analyses can be found in [14, 15].

2 Experimental setup, data samples, and event simulation

The central feature of the CMS apparatus is a superconducting solenoid, of 6 m internal diameter, providing a field of 3.8 T. Within the field volume are the silicon pixel and strip tracker [16], the crystal electromagnetic calorimeter and the brass-scintillator hadron calorimeter. Muons are measured in gas-ionization detectors embedded in the steel return yokes [17]. In the barrel there is a Drift Tube (DT) system interspersed with Resistive Plate Chambers (RPCs), and in the endcaps there is a Cathode Strip Chamber (CSC) system, also interspersed with RPCs. In addition to the barrel and endcap detectors, CMS has extensive forward calorimetry. A detailed description of CMS can be found in [9].

The CMS detector is installed in an underground cavern, with the center of the detector 89 m below Earth's surface, and 420 m above sea level. The location is $46^\circ\,18.57'$ north latitude and $6^\circ\,4.62'$ east longitude. The upper 50 m of the material above CMS consists of moraines, followed by 20 m of molasse rock. A large access shaft with a diameter of 20.5 m rises vertically to the surface, and is offset from the center of CMS by 14 m along the beam direction. It is covered by a movable concrete plate of 2.25 m thickness. Thus, depending on the point of impact on CMS, the total material traversed by close-to-vertical muons changes from approximately 6 to 175 meters of water equivalent.

The CMS experiment uses a right-handed coordinate system, with the origin at the nominal proton-proton collision point, the x axis pointing towards the center of the LHC ring, the y axis pointing upwards (perpendicular to the LHC plane), and the z axis pointing along the anticlockwise beam-direction, at geographic azimuth 280.8° (approximately west). The angle between the CMS y axis and the zenith direction is 0.8°. This small difference is neglected in the analysis, and the angle of the muons relative to the y axis is used to represent the zenith angle θ_z.

At the center of the detector, the magnetic field is parallel to the central axis of the solenoid, which is aligned with the z axis. Muon momenta are reconstructed by measuring the curvature of the muon trajectory projected on the xy plane, which yields the component of muon momentum transverse to the z axis, $p_{\mathrm{T}} = p \sin\theta$, where θ is the polar angle with respect to the z axis. This configuration is favourable for the reconstruction of atmospheric muons, providing a strong magnetic bending for muons traversing the detector, at any incident azimuthal angle ϕ around the z axis. Full tracking of muons is available in the polar angle range $10^\circ < \theta < 170^\circ$.

CMS collected cosmic ray data in several runs during the final years of detector construction and commissioning. Data from the Magnet Test and Cosmic Challenge in 2006 (MTCC) [12] and the Cosmic Run At Four Tesla in 2008 (CRAFT08) [13] are used in the analysis reported here.

In August 2006 the CMS detector was pre-assembled on the surface before being lowered into the cavern. In this configuration no material above the detector was present, apart from the thin metal roof of the assembly hall. A small fraction of each of the subdetectors was instrumented and operating at the time. The details of the MTCC setup are described in [12, 14]. About 25 million cosmic-muon events were recorded during the first phase of the MTCC with the magnet at a number of field values ranging from 3.67 to 4.00 T.

The CRAFT08 campaign was a sustained data-taking exercise in October and November 2008 with the CMS detector fully assembled in its final underground position. The full detector, ready for collecting data from LHC, participated in the run, with the magnet at the nominal field of 3.8 T. Approximately 270 million cosmic-muon events were recorded.

Single cosmic muons are simulated using the Monte Carlo event generator CMSCGEN [18, 19], which makes use of parameterizations of the distributions of the muon energy and incidence angle based on the air shower program CORSIKA [20]. The CMS detector response is simulated using the GEANT4 program [21], which takes into account the effects of energy loss, multiple scattering, and showering in the detector. A map [19] describing the various materials between the Earth's surface and the CMS detector is used to obtain the average expected energy loss of simulated muons as a function of their energy, impact point, and incidence direction at the surface.

3 Cosmic-muon reconstruction

Muon tracking in CMS can be performed with the all-silicon tracker at the heart of the detector, and with either three or four stations of muon chambers installed outside the solenoid, sandwiched between steel layers serving both as hadron absorbers and as a return yoke for the magnetic field.

Three types of muon-track reconstruction were designed for cosmic muons not originating from an LHC proton-proton collision [22]: a standalone-muon track includes only hits from the muon detectors; a tracker track includes only hits from the silicon tracker; and a global-muon track combines hits from the muon system and the silicon tracker in a combined track fit. For a cosmic muon that crosses the whole CMS detector, illustrated in Fig. 1 (top), each of the above types of tracks can be fitted separately in the top and bottom halves of CMS. Alternatively, a single track fit can be made including hits from the top and bottom halves of CMS. The direction of the muon is assumed to be downwards, and the muon charge is defined accordingly.

The analysis based on 2006 MTCC data uses standalone muons. The reduced detector setup

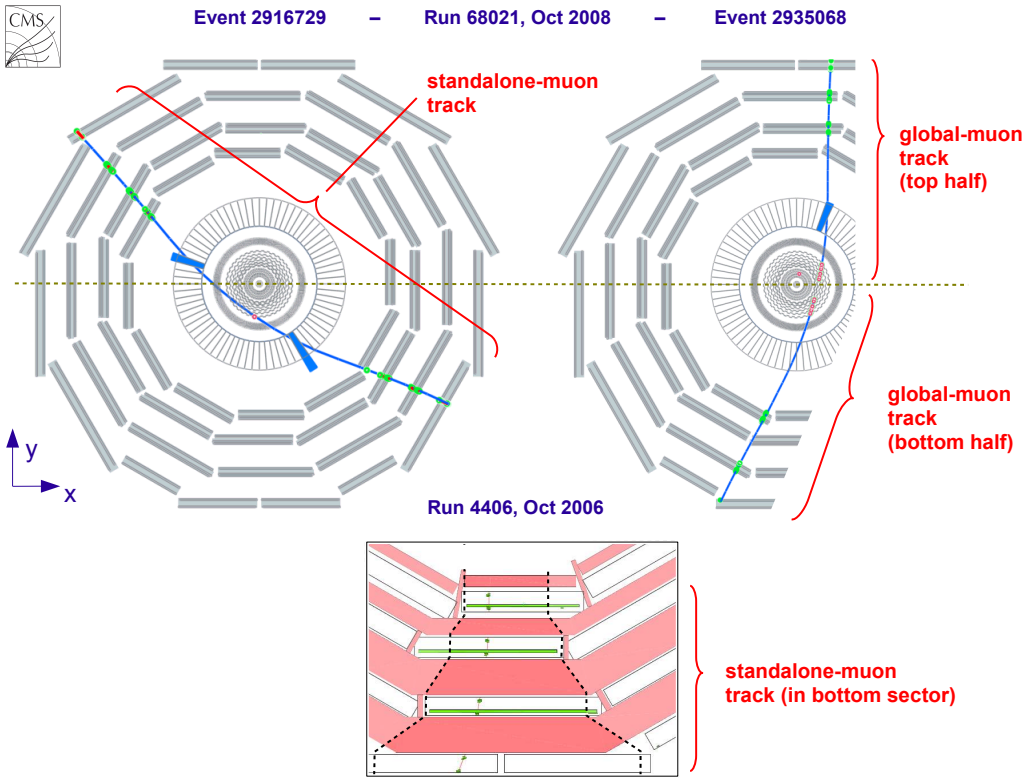

Figure 1: Cosmic-ray muons crossing the CMS detector. The upper two pictures display muons from 2008 underground data, leaving signals in the muon system, tracking detectors and calorimeters. A standalone track (top left) and a pair of global half-tracks (top right) are shown. The bottom plot depicts a muon from 2006 surface data crossing the muon chambers at the bottom of CMS.

used in the MTCC was just a fraction of the bottom half of the complete detector, depicted in Fig. 1 (bottom). Since the muons were measured only in one half of the detector, the momentum resolution is poorer than in the standalone-muon analysis using the complete detector. Having the detector on the surface, however, permitted the collection of a large number of low-momentum muons, down to a momentum of 5 GeV/c, allowing for a precise measurement of the charge ratio in the low-momentum range.

Two analyses based on the 2008 CRAFT08 underground data are performed, one using standalone muons and the other using global muons. The underground global-muon analysis (GLB) profits from the excellent momentum resolution and charge determination of global-muon tracks, but requires that the muon passes through the silicon tracker. The underground standalone-muon analysis (STA) profits from the larger acceptance of the muon chambers and yields approximately eight times as many muons as the global-muon analysis. In a standalone cosmic-muon fit spanning the whole diameter of the muon detector (Fig. 1), the momentum resolution is significantly improved compared to a standalone fit using only half the detector. The improvement varies from a factor of four at low momentum to more than a factor of ten for momenta above 100 GeV/c [22].

The "maximum detectable momentum", p_{mdm}, defined as the momentum for which the curvature of a muon track is measured to be one standard deviation away from zero, is around 200 GeV/c for standalone-muon tracks in one half of the detector, around 10 TeV/c for standalone-

muon tracks traversing the entire detector, and in excess of 20 TeV/c for global-muon tracks. The distribution of the transverse momentum ($p_{\mathrm{T}}^{\mathrm{PCA}}$), calculated at the point of closest approach (PCA) to the nominal proton-proton collision point taking into account the energy loss in the detector, is depicted in Fig. 2 (a) for the muons selected in the global and standalone-muon underground analyses.

The redundancy of the different tracking systems in the complete CMS detector allows the determination of the momentum resolution and rate of charge misassignment (the fraction of muons reconstructed with incorrect charge) directly in data. In the global-muon analysis, the half-difference of the track curvatures measured in the top half and the bottom half of the detector $d_{C_{\mathrm{T}}}$ is used to measure the resolution of the half-sum C_{T}:

$$\begin{aligned} C_{\mathrm{T}} &\equiv \left(\frac{q}{p_{\mathrm{T}}}\right)_{\text{average}} = \frac{1}{2}\left[\left(\frac{q}{p_{\mathrm{T}}}\right)_{\text{top}} + \left(\frac{q}{p_{\mathrm{T}}}\right)_{\text{bottom}}\right], \\ d_{C_{\mathrm{T}}} &\equiv \frac{1}{2}\left[\left(\frac{q}{p_{\mathrm{T}}}\right)_{\text{top}} - \left(\frac{q}{p_{\mathrm{T}}}\right)_{\text{bottom}}\right], \end{aligned} \tag{1}$$

where p_{T} is the transverse momentum and q the charge sign of the muon. Both the core and the tails of the resolution distribution are well reproduced by the $d_{C_{\mathrm{T}}}$ estimator, as demonstrated for simulated events in Fig. 2 (b).

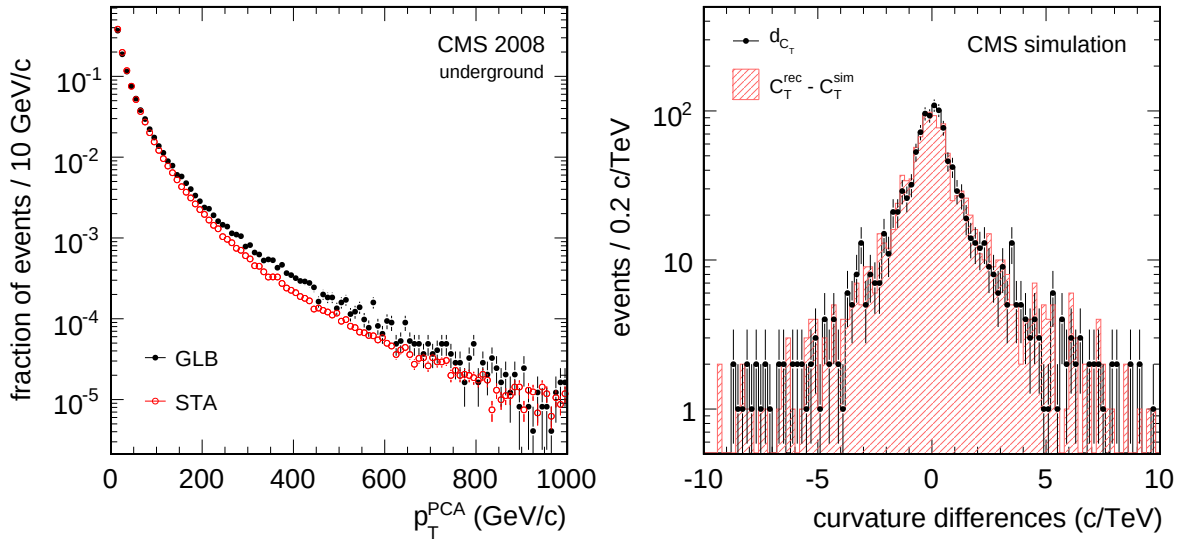

(a) (b)

Figure 2: (a) Normalized muon p_{T} distributions, for the global (closed circles) and standalone-muon analyses (open circles), at the PCA. Differences in the distributions are expected, as the global and standalone-track fits have different momentum resolutions and acceptances. (b) Comparison of the (q/p_{T}) resolution estimate $d_{C_{\mathrm{T}}}$ (closed circles) with the true C_{T} resolution (hatched histogram), obtained from simulated global muons.

In the underground standalone-muon analysis, an independently reconstructed tracker track is available in 40% of the selected events. The comparison of the charge and momentum measured for the tracker track and for the standalone-muon track gives a measure of the tracking resolution both in data and in simulated events.

All three analyses measure the charge ratio in events with a single cosmic ray muon, rejecting events with more than one muon detected.

4 Event selection and analysis

4.1 Analysis of surface data

The cosmic-muon charge ratio was measured by CMS for the first time using MTCC data [14]. For this analysis, only the bottom sector in two (out of five) wheels of the barrel muon system (DT) is used. Selection accepts only muons triggered and reconstructed in a perfectly left-right symmetric fiducial volume with respect to the vertical axis, emphasized in Fig. 1 (bottom), ensuring a charge-symmetric acceptance.

Around 15 million events were recorded in runs with DT triggers and a stable magnetic field above 3.67 T. About 330 000 events pass the fiducial-volume and track-quality selections. The measured muon charge ratio and its statistical uncertainty are displayed in Fig. 3 (a), as a function of the measured muon momentum, before any correction due to detector effects is applied.

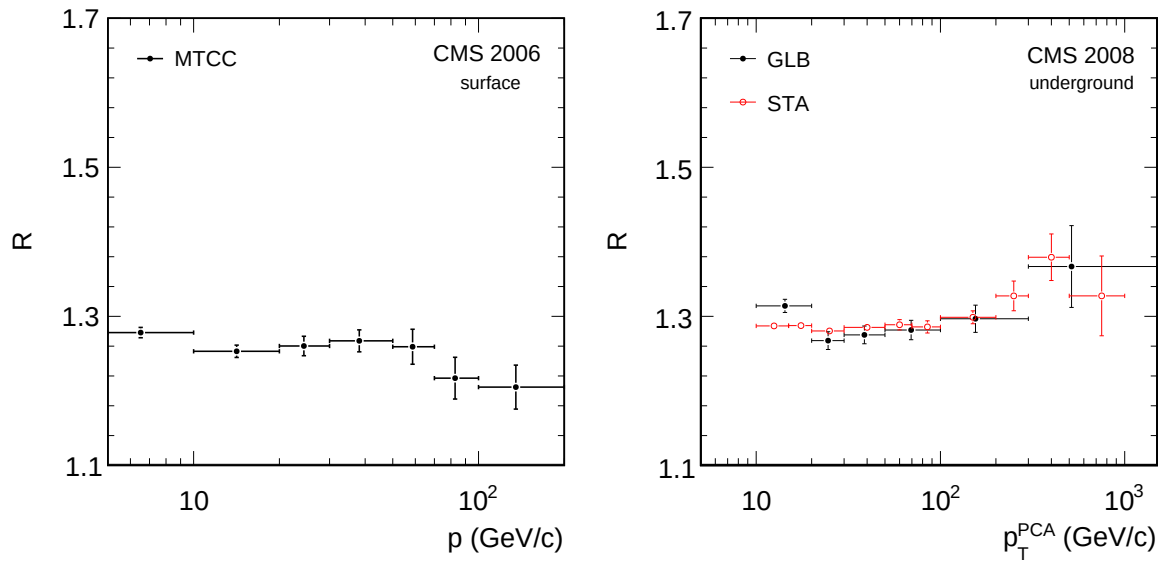

(a) (b)

Figure 3: Uncorrected charge ratio, together with the statistical uncertainty. (a) From 2006 MTCC data, as a function of the measured muon momentum. (b) For the global (closed circles) and standalone-muon analyses (open circles), as a function of the measured p_T at the PCA.

The probability of charge misassignment is small for low-momentum muons. At high momenta, resolution effects increase the chance of charge misassignment thus lowering the measured value of the charge ratio. Only muons with a measured momentum below $p_{\mathrm{mdm}} = 200\,\mathrm{GeV}/c$ are included in the analysis.

4.2 Underground global-muon analysis

The 2008 data were recorded using a single-muon trigger requiring the coincidence of muon hits in at least two muon detector layers. Triggers from the DT or RPC systems in the top or the bottom halves of the detector were accepted. The trigger efficiency is high for muons with

sufficient momentum (a few GeV/c) to penetrate several layers of the steel return yoke [23]. The subsequent event selection is designed to ensure good track quality and high efficiency.

The muon trajectory in each half of the detector is required to contain at least 20 (out of 44 possible) hits in the DT system. Of these 20 hits, at least 3 hits are required to measure the longitudinal coordinate (z), ensuring a good measurement of the polar angle. The muon trajectory is required to contain no hits in the muon or tracker endcaps. The two halves, top and bottom, of each cosmic-muon trajectory are required to be reconstructed as two separate track segments in the silicon tracker, each containing at least 5 hits (out of 12 possible) in the tracker outer barrel system. A loose cut is applied to the normalized χ^2 of each of the two global-muon fits and the polar angles are required to match within $|\Delta \cot\theta| < 0.2$, in order to suppress the small background from multi-muon cosmic shower events. The average transverse momentum of each muon, measured at the PCA, is required to be greater than 10 GeV/c in order to ensure that the muon is able to traverse the entire CMS detector. All selection requirements are applied to the top and bottom muon trajectories.

While the main shaft of the CMS underground area is symmetric with respect to the yz plane, the two auxiliary access shafts are located at asymmetric positions with respect to this plane (cf. Section 2). This causes the geometrical acceptance of the detector to be asymmetric for muons of different charges, since the CMS magnetic field is aligned with the z axis. To remove this effect, muon tracks that cross these auxiliary shafts are not considered in the analysis, nor are muons that cross the mirror images of those regions with respect to the $x = 0$ plane. We refer to this requirement as "symmetric selection".

About 245 000 muons are selected. The muon p_{T} distribution is reported in Fig. 2 (a) for the selected muons. Figure 3 (b) depicts the measured uncorrected charge ratio as a function of $p_{\mathrm{T}}^{\mathrm{PCA}}$.

4.3 Underground standalone-muon analysis

In this analysis the particle trajectory is reconstructed using only the hits in the barrel muon system (DT and RPC). To select muon tracks that are fully contained in the barrel region, events with hits in the endcap CSCs are rejected. A single track is reconstructed using the information from both halves of the detector. Only one standalone muon per event is allowed.

Muon tracks are required to have a transverse momentum, measured at the PCA, larger than 10 GeV/c. At least 45 muon hits (out of 88 possible) are required to be associated with the track. The muon trajectory in the event is also reconstructed as two standalone-muon tracks, one in the upper and one in the lower half of the detector, with more than 20 hits (out of 44 possible) each.

In order to ensure a good track-quality, further selection criteria are applied to the tracks: the normalized χ^2 of each reconstructed muon track must be less than 5, the impact parameter in the xy plane must be less than 100 cm, the track direction at PCA must be vertical within 42° in θ and 60° in ϕ, and the track PCA must lie within the range $|z| < 600$ cm. A "symmetric selection" is also applied as in the global-muon analysis. The number of muons selected is 1.6 million.

The analysis relies on the simulation to correct for charge misassignment and momentum resolution effects, using the data with both a standalone and a tracker track in the event to perform further corrections and estimate systematic uncertainties. From the comparison of tracks reconstructed both in the tracker and in the muon system, the probability of charge misassignment is known to be well below 1% for $p_{\mathrm{T}}^{\mathrm{PCA}} < 0.5$ TeV/c, increasing up to about 1.5% in the highest momentum bin. The difference observed between data and simulation in the subsample of

events that include a tracker track is taken into account to correct the charge misassignment and to assign the related systematic uncertainty, as explained in Section 6.

The muon momentum scale and resolution are determined by comparing the transverse momentum of the standalone-muon track to that of the associated tracker track, and are accurately modeled by the simulation. Therefore the momentum unfolding, which provides an estimate of the true momentum of the muon tracks from the measured momentum, can be based on the simulation. An uncertainty on the momentum resolution for all events, including those without a tracker track, is taken into account as a systematic uncertainty. The momentum scale in the tracker volume is set by the magnetic field, which is known to a precision better than 0.1% [24], as confirmed by additional checks performed with early LHC data [25]. The uncorrected muon charge ratio is shown in Fig. 3 (b) as a function of $p_{\mathrm{T}}^{\mathrm{PCA}}$.

5 Corrections for energy loss and resolution

In order to express the charge ratio measurement as a function of the true momentum at the surface of the Earth, the measured momentum inside the CMS detector has to be corrected for energy lost between the surface of the Earth and the point of measurement. Furthermore, corrections need to be applied for migration of entries from bin to bin due to momentum resolution and for possible misassignment of the muon charge.

5.1 Energy-loss correction

In the MTCC analysis the measured muons are propagated back to the top of CMS, correcting for expected momentum loss and bending in the magnetic field. In addition, the effect of charge misassignment is estimated using simulated events, and a bin-by-bin correction is applied to the measured charge ratio.

For the muons selected in the global and standalone-muon analyses of the 2008 underground data, the average expected energy loss depends strongly on the path followed through the Earth. The underground measurements are corrected for this effect by propagating the trajectory of individual muons back to the Earth's surface, using the same material model as in the simulation (cf. Section 2). Energy loss in matter is about 0.15% higher for μ^+ than for μ^- due to slightly larger ionization losses [7]. This difference is taken into account in the energy-loss correction, but affects the measured charge ratio by less than 0.3% over the entire momentum range.

5.2 Unfolding the momentum spectrum

In the underground data analyses, momentum resolution effects in the detector are corrected using an unfolding technique, applied to the charge-signed inverse momentum $C = q/p$. In this procedure p represents the measured momentum extrapolated to the Earth's surface, where the correlation with the true muon momentum is highest.

The momentum measured at the PCA is propagated first to the top of CMS, accounting for the magnetic field and the amount of material traversed, and then from the top of CMS to the surface of the Earth, following a straight line. The angular resolution of the detector is better than 5 mrad. Only muons with an estimated momentum above 30 GeV/c after this correction are kept in the analyses.

Given a vector of true muon counts N_j^{true} matrix inversion is used to compute the best estimator

$\widetilde{N}_i^{\text{true}}$ from the vector of observed muon counts N_i^{measured}:

$$\begin{aligned} N_i^{\text{measured}} &= \sum_j M_{ij} N_j^{\text{true}} , \\ \widetilde{N}_i^{\text{true}} &= \sum_j \widetilde{M}_{ij}^{-1} N_j^{\text{measured}} . \end{aligned} \tag{2}$$

The migration matrix element M_{ij} is the probability that a muon with true C (C^{true}) in bin j is observed with a measured C (C^{measured}) in bin i. $\widetilde{M}_{ij}$ is an approximation of the exact migration matrix, and is constructed differently for the global and standalone-muon analyses.

In the standalone-muon analysis the migration matrix estimator is extracted by comparing the true momentum to the reconstructed momentum in simulated events.

In the global-muon analysis the approximate migration matrix is derived directly from the data. For each muon, the C values measured in the top and the bottom half of the detector are propagated individually to the Earth's surface. The estimated true C is then defined as $\widetilde{C}^{\text{true}} = (C_{\text{top}} + C_{\text{bottom}})/2$, and the measured values C_{top} and C_{bottom} are used to represent $\widetilde{C}^{\text{measured}}$. They both have the desired property $\widetilde{C}^{\text{measured}} = \widetilde{C}^{\text{true}} \pm d_C$, where d_C is the C resolution estimator, defined as $d_C = (C_{\text{top}} - C_{\text{bottom}})/2$. The matrix $\widetilde{M}_{ij}$ is then populated using these estimated values, for all muons in the selected event sample. As the resolution estimator d_C gives a good representation of the actual resolution of C^{true} (Fig. 2 (b)), this procedure yields a good approximation of the true migration matrix M_{ij}.

In both analyses, variations of the energy loss around the expected value are taken into account in the unfolding procedure by applying an additional 10% Gaussian smearing of the energy-loss correction to the measured momentum when forming the migration matrix. This approximation is based on simulation studies using GEANT4.

The muon counts N_i correspond to the bins of the histograms in which the corrected charge ratio results are presented. The bin boundaries were chosen such that the migration between bins is small. The values of the off-diagonal elements of the migration matrix are below 0.1 in the global-muon analysis and less than 0.2 in the standalone-muon analysis.

The measurement of the charge ratio using 2006 data, corrected for energy loss in the detector and for charge misassignment, is depicted in Fig. 4 as a function of the muon momentum, together with the statistical and systematic uncertainties.

The measurements of the muon charge ratio in the global and standalone-muon analyses of 2008 data are displayed in Fig. 5, as a function of the muon momentum. The "raw" result is based on the final alignment including the scale correction discussed in Section 6. The "corrected" results are based on the unfolding and, for the standalone-muon analysis, include an additional charge-misassignment correction.

6 Systematic uncertainties

Systematic uncertainties arise from reconstruction and instrumental effects that can affect differently the detection efficiency and momentum measurement of μ^+ and μ^-. They are evaluated as a function of the muon momentum at the Earth's surface.

The CMS magnetic field is known with high precision in the region inside the superconducting solenoid, and with less precision in the steel return yoke [24]. Systematic effects on the charge ratio due to the uncertainty on the magnetic field are less than 1%.

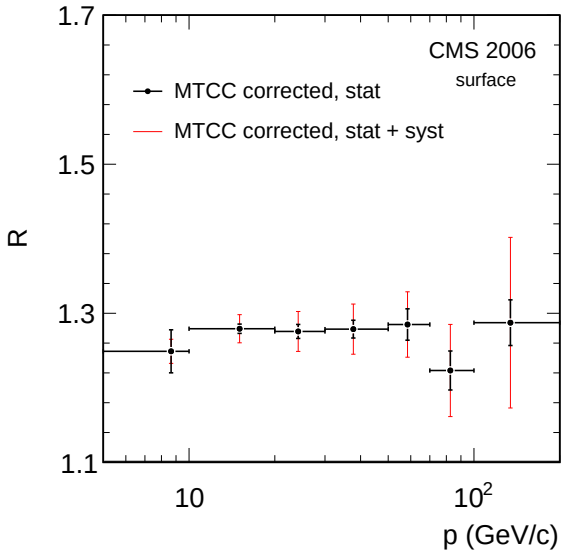

Figure 4: Charge ratio for the surface analysis, as a function of the muon momentum, corrected for energy loss in the detector and for charge misassignment, after propagating the muon track to the entry point in CMS. The thick error bars denote the statistical uncertainty and the thin error bars statistical and systematic uncertainties added in quadrature.

A possible bias in the positive and negative muon rates detected underground, due to asymmetries in detector acceptance and uncertainties in the material densities used in the material map (known within 5%), yields a non-negligible uncertainty on the charge ratio only in the lowest momentum bin. The additional effect of the selection cuts is generally small, well below 1%.

The requirement of a muon trigger in the detector leads to a small difference in efficiency for positive and negative muons, below 1%, which is correlated between the two underground analyses. Both analyses estimate a possible systematic bias induced by the trigger by employing a so-called tag-and-probe technique, using information from both halves of the detector and, in the case of the standalone-muon analysis, information from the independent DT or RPC muon triggers.

In the global-muon analysis the effect of charge misassignment is small, ranging from less than 0.01% at 10 GeV/c to about 1% at 500 GeV/c, and it is corrected by the unfolding procedure, using the data-driven resolution estimator defined in Eq. (1).

In the standalone-muon analysis the charge misassignment correction to the charge ratio, included in the unfolding matrix, is based on simulated events and tested in real data using the subsample of standalone muons with an associated tracker track. A higher rate of charge misassignment is observed in data than in simulation, with a maximum absolute discrepancy of 3% in the highest momentum bin. Since this discrepancy could not be attributed unambiguously to the standalone-muon tracks, a correction is applied equal to 50% of the full effect observed in data, with a systematic uncertainty equal to the correction itself.

The precise alignment of all the tracking-detector components is crucial for accurate reconstruction of high-p_{T} muons, whose trajectories have only a small curvature in the detector. Cosmic muon tracks from the same 2008 data set used for this analysis are employed to perform such an alignment of the silicon tracker and muon system [26, 27]. Possible effects from potential residual misalignment that could lead to momentum migrations and incorrect charge

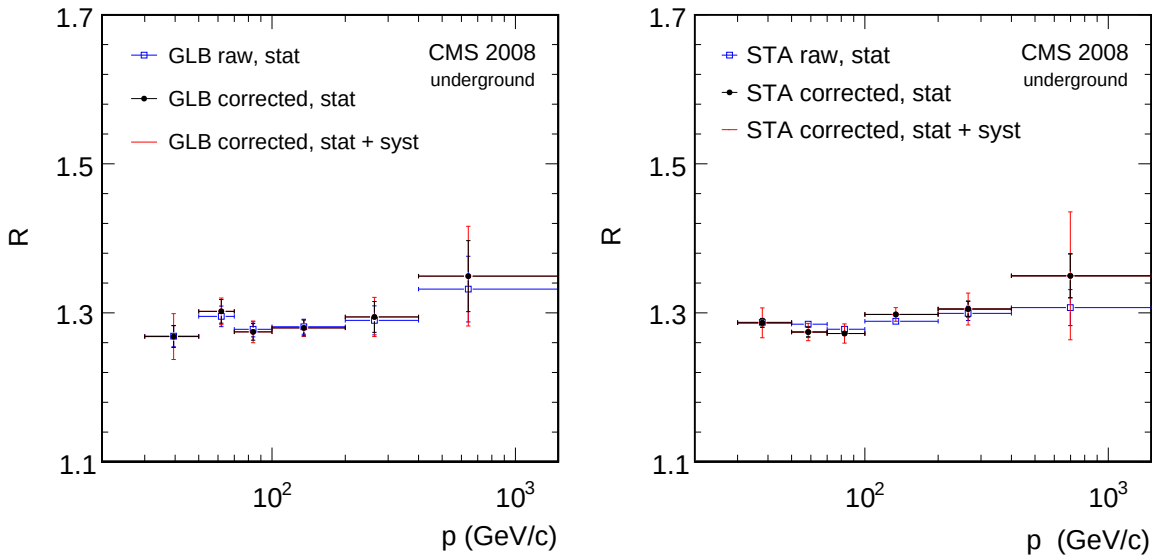

(a) (b)

Figure 5: Muon charge ratio as a function of the muon momentum at the Earth's surface for (a) global and (b) standalone-muon analyses. Open squares indicate the uncorrected ratio, including full alignment. Closed circles show the unfolded charge ratio with statistical errors only. The lines denote the statistical and systematic uncertainties added in quadrature.

assignments are evaluated by studying various realistic missalignment scenarios in data and simulation. Only the two highest momentum bins are potentially affected by misalignment, as expected, yielding a bias in the charge ratio around 1% in the two highest-momentum bins for the global-muon analysis. For the standalone-muon analysis, the effect in the charge ratio is less than 1% up to 400 GeV/c, and around 4% in the highest-momentum bin.

A global deformation of the detector could be missed during the alignment procedures (a so-called "χ^2-invariant" or "weak" mode [28]), and potentially affect the charge ratio. The most problematic deformation would be a mode which caused a constant offset in $q/p_{\mathrm{T}}^{\mathrm{PCA}}$, different from zero, affecting the momentum scale for cosmic muons of opposite charge in opposite directions. A two-parameter fit of the simulated $q/p_{\mathrm{T}}^{\mathrm{PCA}}$ distribution to the data is performed using muons in the range $p_{\mathrm{T}}^{\mathrm{PCA}} > 200\,\mathrm{GeV}/c$, leaving the unknown charge ratio and the $q/p_{\mathrm{T}}^{\mathrm{PCA}}$ offset in the simulation to vary freely in the fit. An offset of $0.043 \pm 0.022\ c/\mathrm{TeV}$ is found. The measured muon momenta are corrected for this offset and its uncertainty is included as an additional systematic uncertainty on R, fully correlated between the two underground measurements, of the order of 1% and 4% respectively in the two highest momentum bins.

In the 2006 MTCC analysis, systematic uncertainties arise mainly from the finite precision of the detector alignment parameters, from the correction of the charge misassignment probability and from the slightly larger uncertainty (∼5%) in the scale of the magnetic field in the steel return yoke.

The total systematic uncertainties in the three analyses are summarized in Table 1, as a function of p at the Earth's surface. The systematic uncertainties have also been evaluated as a function of the vertical momentum component, $p\cos\theta_z$, an observable on which the charge ratio is expected to depend in a simple way [7].

Table 1: Charge ratio R and relative statistical (stat.) and systematic (syst.) uncertainties in bins of p (in GeV/c), for surface data and both analyses of underground data. The relative uncertainties are expressed in %.

p	2006 surface			2008 global-muon			2008 standalone-muon		
range	R	stat.	syst.	R	stat.	syst.	R	stat.	syst.
5 – 10	1.249	2.3	1.3	–	–	–	–	–	–
10 – 20	1.279	0.5	1.5	–	–	–	–	–	–
20 – 30	1.276	0.7	2.1	–	–	–	–	–	–
30 – 50	1.279	0.9	2.6	1.268	1.2	2.1	1.287	0.5	1.5
50 – 70	1.285	1.6	3.4	1.302	1.2	0.6	1.274	0.5	0.8
70 – 100	1.223	2.1	5.1	1.274	0.9	0.7	1.272	0.4	0.9
100 – 200	1.287	2.4	8.9	1.280	0.8	0.3	1.298	0.3	0.6
200 – 400	–	–	–	1.295	1.6	1.3	1.305	0.8	1.4
$>$ 400	–	–	–	1.349	3.5	3.5	1.350	2.2	6.0

7 Results

The results of the three analyses are shown in Fig. 6 (a), as a function of the muon momentum. In the region where the results overlap, agreement between them is good, so the individual analyses are combined using a standard prescription [29]. Within each analysis, some systematic uncertainties are assumed to be correlated between momentum bins: trigger efficiency, momentum scale, charge misassignment and asymmetries in the muon losses due to the detector acceptance. In the global and standalone-muon analyses, systematic uncertainties from material densities, event selection, alignment, and magnetic field, are mostly uncorrelated between momentum bins, and are treated as fully uncorrelated. On the other hand, they are correlated between the two analyses.

The combined data points are given in Table 2 as a function of p and $p\cos\theta_z$. They are shown in Fig. 6 (a) as a function of p, and in Fig. 6 (b) as a function of $p\cos\theta_z$.

Table 2: The muon charge ratio R from the combination of all three CMS analyses, as a function of p and $p\cos\theta_z$, in GeV/c, together with the combined statistical and systematic relative uncertainty, in %.

p range	$\langle p \rangle$	R	uncertainty	$p\cos\theta_z$ range	$\langle p\cos\theta_z \rangle$	R	uncertainty
5 – 10	7.0	1.250	2.45	2.5 – 10	5.3	1.274	0.99
10 – 20	13.7	1.277	0.85	10 – 20	13.6	1.251	1.26
20 – 30	24.2	1.276	1.34	20 – 30	24.1	1.262	1.88
30 – 50	37.8	1.279	1.10	30 – 50	37.7	1.292	1.27
50 – 70	58.5	1.275	0.54	50 – 70	58.4	1.267	0.71
70 – 100	82.5	1.275	0.68	70 – 100	82.4	1.289	0.70
100 – 200	134.0	1.292	0.52	100 – 200	133.1	1.292	0.72
200 – 400	265.8	1.308	1.29	200 – 400	264.0	1.330	1.99
$>$ 400	698.0	1.321	3.98	$>$ 400	654.0	1.378	6.04

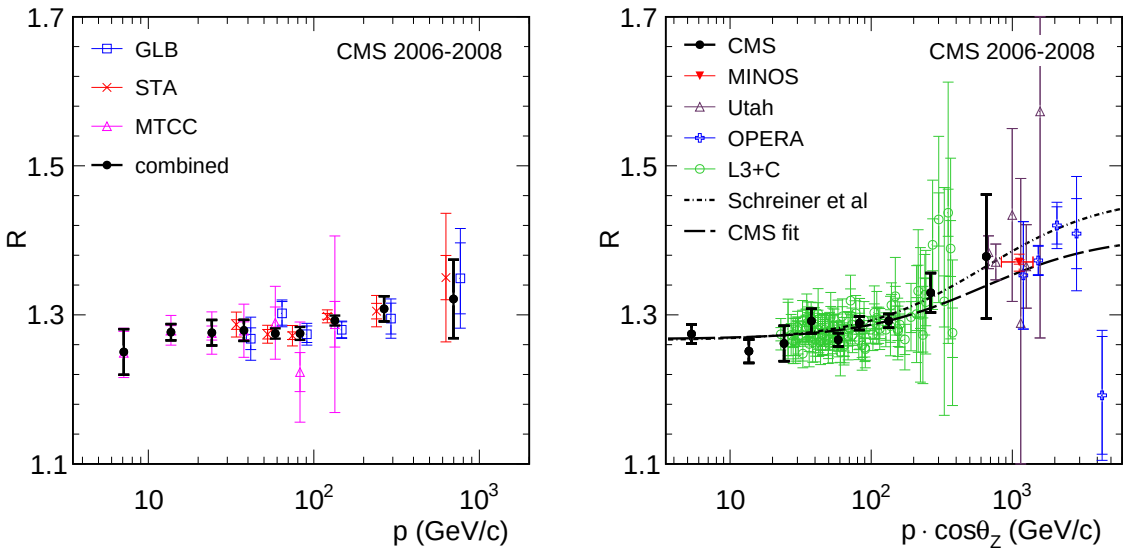

(a) (b)

Figure 6: (a) The three CMS results, and their combination, as a function of the muon momentum. Data points are placed at the bin average, with the points from the standalone and global-muon analyses offset horizontally by ±10% for clarity. (b) The CMS result, as a function of the vertical component of the muon momentum, together with some previous measurements and a fit of the pion-kaon model to the CMS data.

7.1 Charge ratio below 100 GeV/*c*

In the region $p < 100\,\text{GeV}/c$ there are measurements in six p bins. Three bins are covered by all three analyses, with the surface-based MTCC analysis extending the reach to three lower-momentum bins. These twelve data points are combined into a single value of the charge ratio using the same prescription and scenario for correlations as for the overall combination described in the above section. This yields a charge ratio of $1.2766 \pm 0.0032\,(\text{stat.}) \pm 0.0032\,(\text{syst.})$, with a $\chi^2/\text{ndf} = 7.3/11$, in good agreement with previous measurements [2–5] and representing a significant improvement in precision.

Repeating this fit in the $p\cos\theta_z$ region below 100 GeV/c yields a charge ratio of $1.2772 \pm 0.0032\,(\text{stat.}) \pm 0.0036\,(\text{syst.})$, with a $\chi^2/\text{ndf} = 15.3/11$. The higher χ^2/ndf indicates that the data in this $p\cos\theta_z$ region have a lower probability of being consistent with a flat charge ratio. Fitting just the region $p\cos\theta_z < 70$ GeV/c yields a charge ratio of $1.2728 \pm 0.0039\,(\text{stat.}) \pm 0.0040\,(\text{syst.})$ with a $\chi^2/\text{ndf} = 4.0/8$, consistent with the flat charge ratio hypothesis.

7.2 Charge ratio in the 5 GeV/*c* to 1 TeV/*c* momentum range

Considering the full $p\cos\theta_z$ range measured, a rise in the charge ratio is seen, as shown in Fig. 6 (b). Comparing to previous measurements in the same momentum ranges, the CMS results agree well where there is overlap: with the L3+C measurement [5] below 400 GeV/c, and with the UTAH [1], MINOS [6] and OPERA [8] measurements above 400 GeV/c. Measurements by other experiments in the range 5–20 GeV/c [2–5, 30] are not shown in the plot; they are consistent with the constant value fitted in the CMS data.

Models of cosmic ray showers provide an explanation for the rise in charge ratio at higher mo-

mentum. Based on the quark content of protons, and on the observation that primary cosmic ray particles are mostly positive, the ratio π^+/π^- is predicted to be around 1.27 [31]. Due to the phenomena of associated production, the charge ratio of strange particles such as kaons is expected to be even higher.

The expected muon spectrum has been parametrized [32] based on the interactions of primary cosmic ray particles and on the decays of secondary particles, and from this parametrization, the charge ratio can be extracted [7] as a function of the fractions of all pion and kaon decays that yield positive muons, f_π and f_K, respectively. These constants are not known *a priori*, and must be inferred from data.

A fit performed to the combined CMS charge ratio measurement in the entire $p\cos\theta_z$ region, with a fixed relative amount of kaon production [32], yields $f_\pi = 0.553 \pm 0.005$, and $f_K = 0.66 \pm 0.06$, with a $\chi^2/\text{ndf} = 7.8/7$. Figure 6 (b) shows the fit to CMS data only, together with a fit performed on some previous measurements by L3+C and MINOS [7].

8 Conclusions

We have measured the flux ratio of positive- to negative-charge cosmic ray muons, as a function of the muon momentum and its vertical component, using data collected by the CMS experiment in 2006 and 2008. The result is in agreement with previous measurements by underground experiments. This is the most precise measurement of the charge ratio in the momentum region below 0.5 TeV/c. It is also the first physics measurement using muons with the complete CMS detector.

Acknowledgments

We thank the technical and administrative staff at CERN and other CMS institutes. This work was supported by the Austrian Federal Ministry of Science and Research; the Belgium Fonds de la Recherche Scientifique, and Fonds voor Wetenschappelijk Onderzoek; the Brazilian Funding Agencies (CNPq, CAPES, FAPERJ, and FAPESP); the Bulgarian Ministry of Education and Science; CERN; the Chinese Academy of Sciences, Ministry of Science and Technology, and National Natural Science Foundation of China; the Colombian Funding Agency (COLCIENCIAS); the Croatian Ministry of Science, Education and Sport; the Research Promotion Foundation, Cyprus; the Estonian Academy of Sciences and NICPB; the Academy of Finland, Finnish Ministry of Education, and Helsinki Institute of Physics; the Institut National de Physique Nucléaire et de Physique des Particules / CNRS, and Commissariat à l'Énergie Atomique, France; the Bundesministerium für Bildung und Forschung, Deutsche Forschungsgemeinschaft, and Helmholtz-Gemeinschaft Deutscher Forschungszentren, Germany; the General Secretariat for Research and Technology, Greece; the National Scientific Research Foundation, and National Office for Research and Technology, Hungary; the Department of Atomic Energy, and Department of Science and Technology, India; the Institute for Studies in Theoretical Physics and Mathematics, Iran; the Science Foundation, Ireland; the Istituto Nazionale di Fisica Nucleare, Italy; the Korean Ministry of Education, Science and Technology and the World Class University program of NRF, Korea; the Lithuanian Academy of Sciences; the Mexican Funding Agencies (CINVESTAV, CONACYT, SEP, and UASLP-FAI); the Pakistan Atomic Energy Commission; the State Commission for Scientific Research, Poland; the Fundação para a Ciência e a Tecnologia, Portugal; JINR (Armenia, Belarus, Georgia, Ukraine, Uzbekistan); the Ministry of Science and Technologies of the Russian Federation, and Russian Ministry of Atomic Energy; the Ministry of Science and Technological Development of Serbia; the Ministe-

rio de Ciencia e Innovación, and Programa Consolider-Ingenio 2010, Spain; the Swiss Funding Agencies (ETH Board, ETH Zurich, PSI, SNF, UniZH, Canton Zurich, and SER); the National Science Council, Taipei; the Scientific and Technical Research Council of Turkey, and Turkish Atomic Energy Authority; the Science and Technology Facilities Council, UK; the US Department of Energy, and the US National Science Foundation.

Individuals have received support from the Marie-Curie IEF program (European Union); the Leventis Foundation; the A. P. Sloan Foundation; the Alexander von Humboldt Foundation; and the Associazione per lo Sviluppo Scientifico e Tecnologico del Piemonte (Italy).

References

[1] G. K. Ashley, J. W. Keuffel, and M. O. Larson, "Charge ratio of ultra-high-energy cosmic-ray muons", *Phys. Rev. D* **12** (1975), no. 1, 20. doi:10.1103/PhysRevD.12.20.

[2] J. M. Baxendale, C. J. Hume, and M. G. Thompson, "Precise measurement of the sea level muon charge ratio", *J. Phys. G: Nucl. Phys.* **1** (1975) 781. doi:10.1088/0305-4616/1/7/012.

[3] B. C. Rastin, "An accurate measurement of the sea-level muon spectrum within the range 4 to 3000 GeV/c", *J. Phys. G: Nucl. Phys.* **10** (1984) 1629. doi:10.1088/0305-4616/10/11/017.

[4] T. Hebbeker and C. Timmermans, "A compilation of high energy atmospheric muon data at sea level", *Astropart. Phys.* **18** (2002) 107. doi:10.1016/S0927-6505(01)00180-3.

[5] L3 Collaboration, "Measurement of the atmospheric muon spectrum from 20 to 3000 GeV", *Phys. Lett. B* **598** (2004) 15. doi:10.1016/j.physletb.2004.08.003.

[6] MINOS Collaboration, "Measurement of the atmospheric muon charge ratio at TeV energies with MINOS", *Phys. Rev. D* **76** (2007) 052003, arXiv:0705.3815. doi:10.1103/PhysRevD.76.052003.

[7] P. A. Schreiner, J. Reichenbacher, and M. C. Goodman, "Interpretation of the Underground Muon Charge Ratio", *Astropart. Phys.* **32, Issue 1** (2009) 61. doi:10.1016/j.astropartphys.2009.06.002.

[8] OPERA Collaboration, "Measurement of the atmospheric muon charge ratio with the OPERA detector", *submitted to Eur. Phys. J.* **C** (2010) arXiv:1003.1907v1.

[9] CMS Collaboration, "The CMS Experiment at the CERN LHC", *JINST* **3** (2008) S08004. doi:10.1088/1748-0221/3/08/S08004.

[10] J. Evans and P. Bryant, "LHC Machine", *JINST* **3** (2008) S08001. doi:10.1088/1748-0221/3/08/S08001.

[11] CMS Collaboration, "CMS Physics TDR: Volume II, Physics Performance", *J. Phys. G: Nucl. Part. Phys.* **34** (2007) 995. doi:10.1088/0954-3899/34/6/E01.

[12] CMS Collaboration, "The CMS Magnet Test and Cosmic Challenge", *CMS Note* **2007/005** (2007).

[13] CMS Collaboration, "Commissioning of the CMS experiment and the cosmic run at four tesla", *JINST* **5** (2010) T03001. doi:10.1088/1748-0221/5/03/T03001.

[14] M. Aldaya and P. Garcia-Abia, "Measurement of the charge ratio of cosmic muons using CMS data", *CMS Note* **2008/016** (2008).

[15] CMS Collaboration, "Measurement of the charge asymmetry of atmospheric muons with the CMS detector", *CMS PAS* **MUO-10-001** (2010).

[16] CMS Collaboration, "CMS Tracker Technical Design Report", *CERN/LHCC* **1998-006** (1998).

[17] CMS Collaboration, "CMS Muon Technical Design Report", *CERN/LHCC* **1997-032** (1997).

[18] P. Biallass and T. Hebbeker, "Parametrization of the Cosmic Muon Flux for the Generator CMSCGEN", arXiv:0907.5514v1.

[19] L. Sonnenschein, "Cosmic muons in simulation and measured data (Lepton Photon 09)", *CMS CR* **2010/005** (2010).

[20] D. Heck et al., "CORSIKA, A Monte Carlo to simulate Extensive Air Showers", *Forschungszentrum Karlsruhe, Report FZKA* **6019** (1998).

[21] S. Agostinelli et al., "GEANT4: A simulation toolkit", *Nucl. Inst. Meth. A* **506** (2003) 250. doi:10.1016/S0168-9002(03)01368-8.

[22] CMS Collaboration, "Performance of CMS muon reconstruction in cosmic-ray events", *JINST* **5** (2010) T03022. doi:10.1088/1748-0221/5/03/T03022.

[23] CMS Collaboration, "Performance of the CMS level-1 trigger during commissioning with cosmic rays", *JINST* **5** (2010) T03002. doi:10.1088/1748-0221/5/03/T03002.

[24] CMS Collaboration, "Precise mapping of the magnetic field in the CMS barrel yoke using cosmic rays", *JINST* **5** (2010) T03021. doi:10.1088/1748-0221/5/03/T03021.

[25] CMS Collaboration, "Tracking and Vertexing Results from First Collisions", *CMS PAS* **TRK-10-001** (2010).

[26] CMS Collaboration, "Alignment of the CMS silicon tracker during commissioning with cosmic rays", *JINST* **5** (2010) T03009. doi:10.1088/1748-0221/5/03/T03009.

[27] CMS Collaboration, "Alignment of the CMS muon system with cosmic-ray and beam-halo muons", *JINST* **5** (2010) T03020. doi:10.1088/1748-0221/5/03/T03020.

[28] G. Flucke et al., "CMS silicon tracker alignment strategy with the Millepede II algorithm", *JINST* **3** (2008) P09002. doi:10.1088/1748-0221/3/09/P09002.

[29] L. Lyons, D. Gibaut, and P. Clifford, "How to Combine Correlated Estimates of a Single Physical Quantity", *Nucl. Inst. Meth. A* **270** (1988) 110; A. Valassi, "Combining correlated measurements of several different physical quantities", *Nucl. Inst. Meth. A* **500** (2003) 391.

[30] BESS Collaboration, "Measurements of primary and atmospheric cosmic-ray spectra with the BESS-TeV spectrometer", *Phys. Lett. B* **594** (2004) 35. doi:10.1016/j.physletb.2004.05.019.

[31] G. Fiorentini, V. Naumov, and F. Villante, "Atmospheric neutrino flux supported by recent muon experiments", *Phys. Lett. B* **510** (2001) 173. doi:10.1016/S0370-2693(01)00572-X.

[32] T. Gaisser, "Cosmic Rays and Particle Physics", *Cambridge University Press* 1990.

A The CMS Collaboration

Yerevan Physics Institute, Yerevan, Armenia
V. Khachatryan, A.M. Sirunyan, A. Tumasyan

Institut für Hochenergiephysik der OeAW, Wien, Austria
W. Adam, T. Bergauer, M. Dragicevic, J. Erö, C. Fabjan, M. Friedl, R. Frühwirth, V.M. Ghete, J. Hammer[1], S. Hänsel, M. Hoch, N. Hörmann, J. Hrubec, M. Jeitler, G. Kasieczka, W. Kiesenhofer, M. Krammer, D. Liko, I. Mikulec, M. Pernicka, H. Rohringer, R. Schöfbeck, J. Strauss, A. Taurok, F. Teischinger, W. Waltenberger, G. Walzel, E. Widl, C.-E. Wulz

National Centre for Particle and High Energy Physics, Minsk, Belarus
V. Mossolov, N. Shumeiko, J. Suarez Gonzalez

Universiteit Antwerpen, Antwerpen, Belgium
L. Benucci, L. Ceard, E.A. De Wolf, M. Hashemi, X. Janssen, T. Maes, L. Mucibello, S. Ochesanu, B. Roland, R. Rougny, M. Selvaggi, H. Van Haevermaet, P. Van Mechelen, N. Van Remortel

Vrije Universiteit Brussel, Brussel, Belgium
V. Adler, S. Beauceron, S. Blyweert, J. D'Hondt, O. Devroede, A. Kalogeropoulos, J. Maes, M. Maes, S. Tavernier, W. Van Doninck, P. Van Mulders, I. Villella

Université Libre de Bruxelles, Bruxelles, Belgium
E.C. Chabert, O. Charaf, B. Clerbaux, G. De Lentdecker, V. Dero, A.P.R. Gay, G.H. Hammad, P.E. Marage, C. Vander Velde, P. Vanlaer, J. Wickens

Ghent University, Ghent, Belgium
S. Costantini, M. Grunewald, B. Klein, A. Marinov, D. Ryckbosch, F. Thyssen, M. Tytgat, L. Vanelderen, P. Verwilligen, S. Walsh, N. Zaganidis

Université Catholique de Louvain, Louvain-la-Neuve, Belgium
S. Basegmez, G. Bruno, J. Caudron, J. De Favereau De Jeneret, C. Delaere, P. Demin, D. Favart, A. Giammanco, G. Grégoire, J. Hollar, V. Lemaitre, O. Militaru, S. Ovyn, D. Pagano, A. Pin, K. Piotrzkowski[1], L. Quertenmont, N. Schul

Université de Mons, Mons, Belgium
N. Beliy, T. Caebergs, E. Daubie

Centro Brasileiro de Pesquisas Fisicas, Rio de Janeiro, Brazil
G.A. Alves, M. Carneiro, M.E. Pol, M.H.G. Souza

Universidade do Estado do Rio de Janeiro, Rio de Janeiro, Brazil
W. Carvalho, E.M. Da Costa, D. De Jesus Damiao, C. De Oliveira Martins, S. Fonseca De Souza, L. Mundim, V. Oguri, A. Santoro, S.M. Silva Do Amaral, A. Sznajder, F. Torres Da Silva De Araujo

Instituto de Fisica Teorica, Universidade Estadual Paulista, Sao Paulo, Brazil
F.A. Dias, M.A.F. Dias, T.R. Fernandez Perez Tomei, E. M. Gregores[2], F. Marinho, S.F. Novaes, Sandra S. Padula

Institute for Nuclear Research and Nuclear Energy, Sofia, Bulgaria
N. Darmenov[1], L. Dimitrov, V. Genchev[1], P. Iaydjiev, S. Piperov, S. Stoykova, G. Sultanov, R. Trayanov, I. Vankov

University of Sofia, Sofia, Bulgaria
M. Dyulendarova, R. Hadjiiska, V. Kozhuharov, L. Litov, E. Marinova, M. Mateev, B. Pavlov, P. Petkov

Institute of High Energy Physics, Beijing, China
J.G. Bian, G.M. Chen, H.S. Chen, C.H. Jiang, D. Liang, S. Liang, J. Wang, J. Wang, X. Wang, Z. Wang, M. Yang, J. Zang, Z. Zhang

State Key Lab. of Nucl. Phys. and Tech., Peking University, Beijing, China
Y. Ban, S. Guo, Z. Hu, Y. Mao, S.J. Qian, H. Teng, B. Zhu

Universidad de Los Andes, Bogota, Colombia
A. Cabrera, C.A. Carrillo Montoya, B. Gomez Moreno, A.A. Ocampo Rios, A.F. Osorio Oliveros, J.C. Sanabria

Technical University of Split, Split, Croatia
N. Godinovic, D. Lelas, K. Lelas, R. Plestina[3], D. Polic, I. Puljak

University of Split, Split, Croatia
Z. Antunovic, M. Dzelalija

Institute Rudjer Boskovic, Zagreb, Croatia
V. Brigljevic, S. Duric, K. Kadija, S. Morovic

University of Cyprus, Nicosia, Cyprus
A. Attikis, R. Fereos, M. Galanti, J. Mousa, C. Nicolaou, A. Papadakis, F. Ptochos, P.A. Razis, H. Rykaczewski, D. Tsiakkouri, Z. Zinonos

Academy of Scientific Research and Technology of the Arab Republic of Egypt, Egyptian Network of High Energy Physics, Cairo, Egypt
M.A. Mahmoud[4]

National Institute of Chemical Physics and Biophysics, Tallinn, Estonia
A. Hektor, M. Kadastik, K. Kannike, M. Müntel, M. Raidal, L. Rebane

Department of Physics, University of Helsinki, Helsinki, Finland
V. Azzolini, P. Eerola

Helsinki Institute of Physics, Helsinki, Finland
S. Czellar, J. Härkönen, A. Heikkinen, V. Karimäki, R. Kinnunen, J. Klem, M.J. Kortelainen, T. Lampén, K. Lassila-Perini, S. Lehti, T. Lindén, P. Luukka, T. Mäenpää, E. Tuominen, J. Tuominiemi, E. Tuovinen, D. Ungaro, L. Wendland

Lappeenranta University of Technology, Lappeenranta, Finland
K. Banzuzi, A. Korpela, T. Tuuva

Laboratoire d'Annecy-le-Vieux de Physique des Particules, IN2P3-CNRS, Annecy-le-Vieux, France
D. Sillou

DSM/IRFU, CEA/Saclay, Gif-sur-Yvette, France
M. Besancon, M. Dejardin, D. Denegri, J. Descamps, B. Fabbro, J.L. Faure, F. Ferri, S. Ganjour, F.X. Gentit, A. Givernaud, P. Gras, G. Hamel de Monchenault, P. Jarry, E. Locci, J. Malcles, M. Marionneau, L. Millischer, J. Rander, A. Rosowsky, D. Rousseau, M. Titov, P. Verrecchia

Laboratoire Leprince-Ringuet, Ecole Polytechnique, IN2P3-CNRS, Palaiseau, France
S. Baffioni, L. Bianchini, M. Bluj[5], C. Broutin, P. Busson, C. Charlot, L. Dobrzynski, S. Elgammal,

R. Granier de Cassagnac, M. Haguenauer, A. Kalinowski, P. Miné, P. Paganini, D. Sabes, Y. Sirois, C. Thiebaux, A. Zabi

Institut Pluridisciplinaire Hubert Curien, Université de Strasbourg, Université de Haute Alsace Mulhouse, CNRS/IN2P3, Strasbourg, France
J.-L. Agram[6], A. Besson, D. Bloch, D. Bodin, J.-M. Brom, M. Cardaci, E. Conte[6], F. Drouhin[6], C. Ferro, J.-C. Fontaine[6], D. Gelé, U. Goerlach, S. Greder, P. Juillot, M. Karim[6], A.-C. Le Bihan, Y. Mikami, J. Speck, P. Van Hove

Centre de Calcul de l'Institut National de Physique Nucleaire et de Physique des Particules (IN2P3), Villeurbanne, France
F. Fassi, D. Mercier

Université de Lyon, Université Claude Bernard Lyon 1, CNRS-IN2P3, Institut de Physique Nucléaire de Lyon, Villeurbanne, France
C. Baty, N. Beaupere, M. Bedjidian, O. Bondu, G. Boudoul, D. Boumediene, H. Brun, N. Chanon, R. Chierici, D. Contardo, P. Depasse, H. El Mamouni, J. Fay, S. Gascon, B. Ille, T. Kurca, T. Le Grand, M. Lethuillier, L. Mirabito, S. Perries, V. Sordini, S. Tosi, Y. Tschudi, P. Verdier, H. Xiao

E. Andronikashvili Institute of Physics, Academy of Science, Tbilisi, Georgia
V. Roinishvili

RWTH Aachen University, I. Physikalisches Institut, Aachen, Germany
G. Anagnostou, M. Edelhoff, L. Feld, N. Heracleous, O. Hindrichs, R. Jussen, K. Klein, J. Merz, N. Mohr, A. Ostapchuk, A. Perieanu, F. Raupach, J. Sammet, S. Schael, D. Sprenger, H. Weber, M. Weber, B. Wittmer

RWTH Aachen University, III. Physikalisches Institut A, Aachen, Germany
O. Actis, M. Ata, W. Bender, P. Biallass, M. Erdmann, J. Frangenheim, T. Hebbeker, A. Hinzmann, K. Hoepfner, C. Hof, M. Kirsch, T. Klimkovich, P. Kreuzer[1], D. Lanske[†], C. Magass, M. Merschmeyer, A. Meyer, P. Papacz, H. Pieta, H. Reithler, S.A. Schmitz, L. Sonnenschein, M. Sowa, J. Steggemann, D. Teyssier, C. Zeidler

RWTH Aachen University, III. Physikalisches Institut B, Aachen, Germany
M. Bontenackels, M. Davids, M. Duda, G. Flügge, H. Geenen, M. Giffels, W. Haj Ahmad, D. Heydhausen, T. Kress, Y. Kuessel, A. Linn, A. Nowack, L. Perchalla, O. Pooth, P. Sauerland, A. Stahl, M. Thomas, D. Tornier, M.H. Zoeller

Deutsches Elektronen-Synchrotron, Hamburg, Germany
M. Aldaya Martin, W. Behrenhoff, U. Behrens, M. Bergholz, K. Borras, A. Campbell, E. Castro, D. Dammann, G. Eckerlin, A. Flossdorf, G. Flucke, A. Geiser, J. Hauk, H. Jung, M. Kasemann, I. Katkov, C. Kleinwort, H. Kluge, A. Knutsson, E. Kuznetsova, W. Lange, W. Lohmann, R. Mankel, M. Marienfeld, I.-A. Melzer-Pellmann, A.B. Meyer, J. Mnich, A. Mussgiller, J. Olzem, A. Parenti, A. Raspereza, R. Schmidt, T. Schoerner-Sadenius, N. Sen, M. Stein, J. Tomaszewska, D. Volyanskyy, C. Wissing

University of Hamburg, Hamburg, Germany
C. Autermann, J. Draeger, D. Eckstein, H. Enderle, U. Gebbert, K. Kaschube, G. Kaussen, R. Klanner, B. Mura, S. Naumann-Emme, F. Nowak, C. Sander, H. Schettler, P. Schleper, M. Schröder, T. Schum, J. Schwandt, A.K. Srivastava, H. Stadie, G. Steinbrück, J. Thomsen, R. Wolf

Institut für Experimentelle Kernphysik, Karlsruhe, Germany
J. Bauer, V. Buege, A. Cakir, T. Chwalek, D. Daeuwel, W. De Boer, A. Dierlamm, G. Dirkes, M. Feindt, J. Gruschke, C. Hackstein, F. Hartmann, M. Heinrich, H. Held, K.H. Hoffmann, S. Honc, T. Kuhr, D. Martschei, S. Mueller, Th. Müller, M. Niegel, O. Oberst, A. Oehler, J. Ott, T. Peiffer, D. Piparo, G. Quast, K. Rabbertz, F. Ratnikov, M. Renz, A. Sabellek, C. Saout[1], A. Scheurer, P. Schieferdecker, F.-P. Schilling, G. Schott, H.J. Simonis, F.M. Stober, D. Troendle, J. Wagner-Kuhr, M. Zeise, V. Zhukov[7], E.B. Ziebarth

Institute of Nuclear Physics "Demokritos", Aghia Paraskevi, Greece
G. Daskalakis, T. Geralis, A. Kyriakis, D. Loukas, I. Manolakos, A. Markou, C. Markou, C. Mavrommatis, E. Petrakou

University of Athens, Athens, Greece
L. Gouskos, P. Katsas, A. Panagiotou[1]

University of Ioánnina, Ioánnina, Greece
I. Evangelou, P. Kokkas, N. Manthos, I. Papadopoulos, V. Patras, F.A. Triantis

KFKI Research Institute for Particle and Nuclear Physics, Budapest, Hungary
A. Aranyi, G. Bencze, L. Boldizsar, G. Debreczeni, C. Hajdu[1], D. Horvath[8], A. Kapusi, K. Krajczar[9], A. Laszlo, F. Sikler, G. Vesztergombi[9]

Institute of Nuclear Research ATOMKI, Debrecen, Hungary
N. Beni, J. Molnar, J. Palinkas, Z. Szillasi[1], V. Veszpremi

University of Debrecen, Debrecen, Hungary
P. Raics, Z.L. Trocsanyi, B. Ujvari

Panjab University, Chandigarh, India
S. Bansal, S.B. Beri, V. Bhatnagar, M. Jindal, M. Kaur, J.M. Kohli, M.Z. Mehta, N. Nishu, L.K. Saini, A. Sharma, R. Sharma, A.P. Singh, J.B. Singh, S.P. Singh

University of Delhi, Delhi, India
S. Ahuja, S. Bhattacharya[10], S. Chauhan, B.C. Choudhary, P. Gupta, S. Jain, S. Jain, A. Kumar, K. Ranjan, R.K. Shivpuri

Bhabha Atomic Research Centre, Mumbai, India
R.K. Choudhury, D. Dutta, S. Kailas, S.K. Kataria, A.K. Mohanty, L.M. Pant, P. Shukla, P. Suggisetti

Tata Institute of Fundamental Research - EHEP, Mumbai, India
T. Aziz, M. Guchait[11], A. Gurtu, M. Maity[12], D. Majumder, G. Majumder, K. Mazumdar, G.B. Mohanty, A. Saha, K. Sudhakar, N. Wickramage

Tata Institute of Fundamental Research - HECR, Mumbai, India
S. Banerjee, S. Dugad, N.K. Mondal

Institute for Studies in Theoretical Physics & Mathematics (IPM), Tehran, Iran
H. Arfaei, H. Bakhshiansohi, A. Fahim, A. Jafari, M. Mohammadi Najafabadi, S. Paktinat Mehdiabadi, B. Safarzadeh, M. Zeinali

INFN Sezione di Bari [a], Università di Bari [b], Politecnico di Bari [c], Bari, Italy
M. Abbrescia[a,b], L. Barbone[a], A. Colaleo[a], D. Creanza[a,c], N. De Filippis[a], M. De Palma[a,b], A. Dimitrov[a], F. Fedele[a], L. Fiore[a], G. Iaselli[a,c], L. Lusito[a,b,1], G. Maggi[a,c], M. Maggi[a], N. Manna[a,b], B. Marangelli[a,b], S. My[a,c], S. Nuzzo[a,b], G.A. Pierro[a], A. Pompili[a,b], G. Pugliese[a,c], F. Romano[a,c], G. Roselli[a,b], G. Selvaggi[a,b], L. Silvestris[a], R. Trentadue[a], S. Tupputi[a,b], G. Zito[a]

INFN Sezione di Bologna [a], Università di Bologna [b], Bologna, Italy
G. Abbiendi[a], A.C. Benvenuti[a], D. Bonacorsi[a], S. Braibant-Giacomelli[a,b], P. Capiluppi[a,b], A. Castro[a,b], F.R. Cavallo[a], G. Codispoti[a,b], M. Cuffiani[a,b], G.M. Dallavalle[a,1], F. Fabbri[a], A. Fanfani[a,b], D. Fasanella[a], M. Giunta[a,1], C. Grandi[a], S. Marcellini[a], G. Masetti[a,b], A. Montanari[a], F. Odorici[a], A. Perrotta[a], A.M. Rossi[a,b], T. Rovelli[a,b], G. Siroli[a,b], R. Travaglini[a,b]

INFN Sezione di Catania [a], Università di Catania [b], Catania, Italy
S. Albergo[a,b], G. Cappello[a,b], M. Chiorboli[a,b], S. Costa[a,b], A. Tricomi[a,b], C. Tuve[a]

INFN Sezione di Firenze [a], Università di Firenze [b], Firenze, Italy
G. Barbagli[a], G. Broccolo[a,b], V. Ciulli[a,b], C. Civinini[a], R. D'Alessandro[a,b], E. Focardi[a,b], S. Frosali[a,b], E. Gallo[a], C. Genta[a,b], P. Lenzi[a,b,1], M. Meschini[a], S. Paoletti[a], G. Sguazzoni[a], A. Tropiano[a]

INFN Laboratori Nazionali di Frascati, Frascati, Italy
L. Benussi, S. Bianco, S. Colafranceschi[13], F. Fabbri, D. Piccolo

INFN Sezione di Genova, Genova, Italy
P. Fabbricatore, R. Musenich

INFN Sezione di Milano-Biccoca [a], Università di Milano-Bicocca [b], Milano, Italy
A. Benaglia[a,b], G.B. Cerati[a,b,1], F. De Guio[a,b], L. Di Matteo[a,b], A. Ghezzi[a,b,1], P. Govoni[a,b], M. Malberti[a,b,1], S. Malvezzi[a], A. Martelli[a,b,3], A. Massironi[a,b], D. Menasce[a], V. Miccio[a,b], L. Moroni[a], P. Negri[a,b], M. Paganoni[a,b], D. Pedrini[a], S. Ragazzi[a,b], N. Redaelli[a], S. Sala[a], R. Salerno[a,b], T. Tabarelli de Fatis[a,b], V. Tancini[a,b], S. Taroni[a,b]

INFN Sezione di Napoli [a], Università di Napoli "Federico II" [b], Napoli, Italy
S. Buontempo[a], A. Cimmino[a,b], A. De Cosa[a,b,1], M. De Gruttola[a,b,1], F. Fabozzi[a,14], A.O.M. Iorio[a], L. Lista[a], P. Noli[a,b], P. Paolucci[a]

INFN Sezione di Padova [a], Università di Padova [b], Università di Trento (Trento) [c], Padova, Italy
P. Azzi[a], N. Bacchetta[a], P. Bellan[a,b,1], R. Carlin[a,b], P. Checchia[a], E. Conti[a], M. De Mattia[a,b], T. Dorigo[a], U. Dosselli[a], F. Fanzago[a], F. Gasparini[a,b], U. Gasparini[a,b], P. Giubilato[a,b], A. Gresele[a,c], A. Kaminskiy[a,b], S. Lacaprara[a,15], I. Lazzizzera[a,c], M. Margoni[a,b], M. Mazzucato[a], A.T. Meneguzzo[a,b], L. Perrozzi[a], N. Pozzobon[a,b], P. Ronchese[a,b], F. Simonetto[a,b], E. Torassa[a], M. Tosi[a,b], S. Vanini[a,b], P. Zotto[a,b], G. Zumerle[a,b]

INFN Sezione di Pavia [a], Università di Pavia [b], Pavia, Italy
P. Baesso[a,b], U. Berzano[a], C. Riccardi[a,b], P. Torre[a,b], P. Vitulo[a,b], C. Viviani[a,b]

INFN Sezione di Perugia [a], Università di Perugia [b], Perugia, Italy
M. Biasini[a,b], G.M. Bilei[a], B. Caponeri[a,b], L. Fanò[a], P. Lariccia[a,b], A. Lucaroni[a,b], G. Mantovani[a,b], M. Menichelli[a], A. Nappi[a,b], A. Santocchia[a,b], L. Servoli[a], M. Valdata[a], R. Volpe[a,b,1]

INFN Sezione di Pisa [a], Università di Pisa [b], Scuola Normale Superiore di Pisa [c], Pisa, Italy
P. Azzurri[a,c], G. Bagliesi[a], J. Bernardini[a,b,1], T. Boccali[a], R. Castaldi[a], R.T. Dagnolo[a,c], R. Dell'Orso[a], F. Fiori[a,b], L. Foà[a,c], A. Giassi[a], A. Kraan[a], F. Ligabue[a,c], T. Lomtadze[a], L. Martini[a], A. Messineo[a,b], F. Palla[a], F. Palmonari[a], G. Segneri[a], A.T. Serban[a], P. Spagnolo[a,1], R. Tenchini[a,1], G. Tonelli[a,b,1], A. Venturi[a], P.G. Verdini[a]

INFN Sezione di Roma [a], Università di Roma "La Sapienza" [b], Roma, Italy
L. Barone[a,b], F. Cavallari[a,1], D. Del Re[a,b], E. Di Marco[a,b], M. Diemoz[a], D. Franci[a,b], M. Grassi[a], E. Longo[a,b], G. Organtini[a,b], A. Palma[a,b], F. Pandolfi[a,b], R. Paramatti[a,1], S. Rahatlou[a,b,1]

INFN Sezione di Torino [a], Università di Torino [b], Università del Piemonte Orientale (Novara) [c], Torino, Italy
N. Amapane[a,b], R. Arcidiacono[a,b], S. Argiro[a,b], M. Arneodo[a,c], C. Biino[a], C. Botta[a,b], N. Cartiglia[a], R. Castello[a,b], M. Costa[a,b], N. Demaria[a], A. Graziano[a,b], C. Mariotti[a], M. Marone[a,b], S. Maselli[a], E. Migliore[a,b], G. Mila[a,b], V. Monaco[a,b], M. Musich[a,b], M.M. Obertino[a,c], N. Pastrone[a], M. Pelliccioni[a,b,1], A. Romero[a,b], M. Ruspa[a,c], R. Sacchi[a,b], A. Solano[a,b], A. Staiano[a], D. Trocino[a,b], A. Vilela Pereira[a,b,1]

INFN Sezione di Trieste [a], Università di Trieste [b], Trieste, Italy
F. Ambroglini[a,b], S. Belforte[a], F. Cossutti[a], G. Della Ricca[a,b], B. Gobbo[a], D. Montanino[a], A. Penzo[a]

Kyungpook National University, Daegu, Korea
S. Chang, J. Chung, D.H. Kim, G.N. Kim, J.E. Kim, D.J. Kong, H. Park, D.C. Son

Chonnam National University, Institute for Universe and Elementary Particles, Kwangju, Korea
Zero Kim, J.Y. Kim, S. Song

Korea University, Seoul, Korea
B. Hong, H. Kim, J.H. Kim, T.J. Kim, K.S. Lee, D.H. Moon, S.K. Park, H.B. Rhee, K.S. Sim

University of Seoul, Seoul, Korea
M. Choi, S. Kang, H. Kim, C. Park, I.C. Park, S. Park

Sungkyunkwan University, Suwon, Korea
S. Choi, Y. Choi, Y.K. Choi, J. Goh, J. Lee, S. Lee, H. Seo, I. Yu

Vilnius University, Vilnius, Lithuania
M. Janulis, D. Martisiute, P. Petrov, T. Sabonis

Centro de Investigacion y de Estudios Avanzados del IPN, Mexico City, Mexico
H. Castilla Valdez[1], E. De La Cruz Burelo, R. Lopez-Fernandez, A. Sánchez Hernández, L.M. Villaseñor-Cendejas

Universidad Iberoamericana, Mexico City, Mexico
S. Carrillo Moreno

Benemerita Universidad Autonoma de Puebla, Puebla, Mexico
H.A. Salazar Ibarguen

Universidad Autónoma de San Luis Potosí, San Luis Potosí, Mexico
E. Casimiro Linares, A. Morelos Pineda, M.A. Reyes-Santos

University of Auckland, Auckland, New Zealand
P. Allfrey, D. Krofcheck, J. Tam

University of Canterbury, Christchurch, New Zealand
P.H. Butler, T. Signal, J.C. Williams

National Centre for Physics, Quaid-I-Azam University, Islamabad, Pakistan
M. Ahmad, I. Ahmed, M.I. Asghar, H.R. Hoorani, W.A. Khan, T. Khurshid, S. Qazi

Institute of Experimental Physics, Warsaw, Poland
M. Cwiok, W. Dominik, K. Doroba, M. Konecki, J. Krolikowski

Soltan Institute for Nuclear Studies, Warsaw, Poland
T. Frueboes, R. Gokieli, M. Górski, M. Kazana, K. Nawrocki, M. Szleper, G. Wrochna, P. Zalewski

Laboratório de Instrumentação e Física Experimental de Partículas, Lisboa, Portugal
N. Almeida, A. David, P. Faccioli, P.G. Ferreira Parracho, M. Gallinaro, G. Mini, P. Musella, A. Nayak, L. Raposo, P.Q. Ribeiro, J. Seixas, P. Silva, D. Soares, J. Varela[1], H.K. Wöhri

Joint Institute for Nuclear Research, Dubna, Russia
I. Altsybeev, I. Belotelov, P. Bunin, M. Finger, M. Finger Jr., I. Golutvin, A. Kamenev, V. Karjavin, G. Kozlov, A. Lanev, P. Moisenz, V. Palichik, V. Perelygin, S. Shmatov, V. Smirnov, A. Volodko, A. Zarubin

Petersburg Nuclear Physics Institute, Gatchina (St Petersburg), Russia
N. Bondar, V. Golovtsov, Y. Ivanov, V. Kim, P. Levchenko, I. Smirnov, V. Sulimov, L. Uvarov, S. Vavilov, A. Vorobyev

Institute for Nuclear Research, Moscow, Russia
Yu. Andreev, S. Gninenko, N. Golubev, M. Kirsanov, N. Krasnikov, V. Matveev, A. Pashenkov, A. Toropin, S. Troitsky

Institute for Theoretical and Experimental Physics, Moscow, Russia
V. Epshteyn, V. Gavrilov, N. Ilina, V. Kaftanov†, M. Kossov[1], A. Krokhotin, S. Kuleshov, A. Oulianov, G. Safronov, S. Semenov, I. Shreyber, V. Stolin, E. Vlasov, A. Zhokin

Moscow State University, Moscow, Russia
E. Boos, M. Dubinin[16], L. Dudko, A. Ershov, A. Gribushin, O. Kodolova, I. Lokhtin, S. Obraztsov, S. Petrushanko, L. Sarycheva, V. Savrin, A. Snigirev

P.N. Lebedev Physical Institute, Moscow, Russia
V. Andreev, I. Dremin, M. Kirakosyan, S.V. Rusakov, A. Vinogradov

State Research Center of Russian Federation, Institute for High Energy Physics, Protvino, Russia
I. Azhgirey, S. Bitioukov, K. Datsko, V. Grishin[1], V. Kachanov, D. Konstantinov, V. Krychkine, V. Petrov, R. Ryutin, S. Slabospitsky, A. Sobol, A. Sytine, L. Tourtchanovitch, S. Troshin, N. Tyurin, A. Uzunian, A. Volkov

Vinca Institute of Nuclear Sciences, Belgrade, Serbia
P. Adzic, M. Djordjevic, D. Krpic[17], D. Maletic, J. Milosevic, J. Puzovic[17]

Centro de Investigaciones Energéticas Medioambientales y Tecnológicas (CIEMAT), Madrid, Spain
M. Aguilar-Benitez, J. Alcaraz Maestre, P. Arce, C. Battilana, E. Calvo, M. Cepeda, M. Cerrada, M. Chamizo Llatas, N. Colino, B. De La Cruz, C. Diez Pardos, C. Fernandez Bedoya, J.P. Fernández Ramos, A. Ferrando, J. Flix, M.C. Fouz, P. Garcia-Abia, O. Gonzalez Lopez, S. Goy Lopez, J.M. Hernandez, M.I. Josa, G. Merino, J. Puerta Pelayo, I. Redondo, L. Romero, J. Santaolalla, C. Willmott

Universidad Autónoma de Madrid, Madrid, Spain
C. Albajar, J.F. de Trocóniz

Universidad de Oviedo, Oviedo, Spain
J. Cuevas, J. Fernandez Menendez, I. Gonzalez Caballero, L. Lloret Iglesias, J.M. Vizan Garcia

Instituto de Física de Cantabria (IFCA), CSIC-Universidad de Cantabria, Santander, Spain
I.J. Cabrillo, A. Calderon, S.H. Chuang, I. Diaz Merino, C. Diez Gonzalez, J. Duarte Campderros, M. Fernandez, G. Gomez, J. Gonzalez Sanchez, R. Gonzalez Suarez, C. Jorda, P. Lobelle Pardo, A. Lopez Virto, J. Marco, R. Marco, C. Martinez Rivero, P. Martinez Ruiz del Arbol, F. Matorras, T. Rodrigo, A. Ruiz Jimeno, L. Scodellaro, M. Sobron Sanudo, I. Vila, R. Vilar Cortabitarte

CERN, European Organization for Nuclear Research, Geneva, Switzerland
D. Abbaneo, E. Auffray, P. Baillon, A.H. Ball, D. Barney, F. Beaudette[3], R. Bellan, D. Benedetti, C. Bernet[3], W. Bialas, P. Bloch, A. Bocci, S. Bolognesi, H. Breuker, G. Brona, K. Bunkowski, T. Camporesi, E. Cano, A. Cattai, G. Cerminara, T. Christiansen, J.A. Coarasa Perez, R. Covarelli, B. Curé, T. Dahms, A. De Roeck, A. Elliott-Peisert, W. Funk, A. Gaddi, S. Gennai, H. Gerwig, D. Gigi, K. Gill, D. Giordano, F. Glege, R. Gomez-Reino Garrido, S. Gowdy, L. Guiducci, M. Hansen, C. Hartl, J. Harvey, B. Hegner, C. Henderson, G. Hesketh, H.F. Hoffmann, A. Honma, V. Innocente, P. Janot, P. Lecoq, C. Leonidopoulos, C. Lourenço, A. Macpherson, T. Mäki, L. Malgeri, M. Mannelli, L. Masetti, G. Mavromanolakis, F. Meijers, S. Mersi, E. Meschi, R. Moser, M.U. Mozer, M. Mulders, E. Nesvold[1], L. Orsini, E. Perez, A. Petrilli, A. Pfeiffer, M. Pierini, M. Pimiä, A. Racz, G. Rolandi[18], C. Rovelli[19], M. Rovere, H. Sakulin, C. Schäfer, C. Schwick, I. Segoni, A. Sharma, P. Siegrist, M. Simon, P. Sphicas[20], D. Spiga, M. Spiropulu[16], F. Stöckli, P. Traczyk, P. Tropea, A. Tsirou, G.I. Veres[9], P. Vichoudis, M. Voutilainen, W.D. Zeuner

Paul Scherrer Institut, Villigen, Switzerland
W. Bertl, K. Deiters, W. Erdmann, K. Gabathuler, R. Horisberger, Q. Ingram, H.C. Kaestli, S. König, D. Kotlinski, U. Langenegger, F. Meier, D. Renker, T. Rohe, J. Sibille[21], A. Starodumov[22]

Institute for Particle Physics, ETH Zurich, Zurich, Switzerland
L. Caminada[23], Z. Chen, S. Cittolin, G. Dissertori, M. Dittmar, J. Eugster, K. Freudenreich, C. Grab, A. Hervé, W. Hintz, P. Lecomte, W. Lustermann, C. Marchica[23], P. Meridiani, P. Milenovic[24], F. Moortgat, A. Nardulli, P. Nef, F. Nessi-Tedaldi, L. Pape, F. Pauss, T. Punz, A. Rizzi, F.J. Ronga, L. Sala, A.K. Sanchez, M.-C. Sawley, D. Schinzel, B. Stieger, L. Tauscher†, A. Thea, K. Theofilatos, D. Treille, M. Weber, L. Wehrli, J. Weng

Universität Zürich, Zurich, Switzerland
C. Amsler, V. Chiochia, S. De Visscher, M. Ivova Rikova, B. Millan Mejias, C. Regenfus, P. Robmann, T. Rommerskirchen, A. Schmidt, D. Tsirigkas, L. Wilke

National Central University, Chung-Li, Taiwan
Y.H. Chang, K.H. Chen, W.T. Chen, A. Go, C.M. Kuo, S.W. Li, W. Lin, M.H. Liu, Y.J. Lu, J.H. Wu, S.S. Yu

National Taiwan University (NTU), Taipei, Taiwan
P. Bartalini, P. Chang, Y.H. Chang, Y.W. Chang, Y. Chao, K.F. Chen, W.-S. Hou, Y. Hsiung, K.Y. Kao, Y.J. Lei, S.W. Lin, R.-S. Lu, J.G. Shiu, Y.M. Tzeng, K. Ueno, C.C. Wang, M. Wang, J.T. Wei

Cukurova University, Adana, Turkey
A. Adiguzel, A. Ayhan, M.N. Bakirci, S. Cerci[25], Z. Demir, C. Dozen, I. Dumanoglu, E. Eskut, S. Girgis, G. Gökbulut, Y. Güler, E. Gurpinar, I. Hos, E.E. Kangal, T. Karaman, A. Kayis Topaksu, A. Nart, G. Önengüt, K. Ozdemir, S. Ozturk, A. Polatöz, O. Sahin, O. Sengul, K. Sogut[26], B. Tali, H. Topakli, D. Uzun, L.N. Vergili, M. Vergili, C. Zorbilmez

Middle East Technical University, Physics Department, Ankara, Turkey
I.V. Akin, T. Aliev, S. Bilmis, M. Deniz, H. Gamsizkan, A.M. Guler, K. Ocalan, A. Ozpineci, M. Serin, R. Sever, U.E. Surat, E. Yildirim, M. Zeyrek

Bogaziçi University, Department of Physics, Istanbul, Turkey
M. Deliomeroglu, D. Demir[27], E. Gülmez, A. Halu, B. Isildak, M. Kaya[28], O. Kaya[28], M. Özbek, S. Ozkorucuklu[29], N. Sonmez[30]

National Scientific Center, Kharkov Institute of Physics and Technology, Kharkov, Ukraine
L. Levchuk

University of Bristol, Bristol, United Kingdom
P. Bell, F. Bostock, J.J. Brooke, T.L. Cheng, D. Cussans, R. Frazier, J. Goldstein, M. Hansen, G.P. Heath, H.F. Heath, C. Hill, B. Huckvale, J. Jackson, L. Kreczko, C.K. Mackay, S. Metson, D.M. Newbold[31], K. Nirunpong, V.J. Smith, S. Ward

Rutherford Appleton Laboratory, Didcot, United Kingdom
L. Basso, K.W. Bell, A. Belyaev, C. Brew, R.M. Brown, B. Camanzi, D.J.A. Cockerill, J.A. Coughlan, K. Harder, S. Harper, B.W. Kennedy, E. Olaiya, D. Petyt, B.C. Radburn-Smith, C.H. Shepherd-Themistocleous, I.R. Tomalin, W.J. Womersley, S.D. Worm

Imperial College, University of London, London, United Kingdom
R. Bainbridge, G. Ball, J. Ballin, R. Beuselinck, O. Buchmuller, D. Colling, N. Cripps, M. Cutajar, G. Davies, M. Della Negra, C. Foudas, J. Fulcher, D. Futyan, A. Guneratne Bryer, G. Hall, Z. Hatherell, J. Hays, G. Iles, G. Karapostoli, L. Lyons, A.-M. Magnan, J. Marrouche, R. Nandi, J. Nash, A. Nikitenko[22], A. Papageorgiou, M. Pesaresi, K. Petridis, M. Pioppi[32], D.M. Raymond, N. Rompotis, A. Rose, M.J. Ryan, C. Seez, P. Sharp, A. Sparrow, M. Stoye, A. Tapper, S. Tourneur, M. Vazquez Acosta, T. Virdee[1], S. Wakefield, D. Wardrope, T. Whyntie

Brunel University, Uxbridge, United Kingdom
M. Barrett, M. Chadwick, J.E. Cole, P.R. Hobson, A. Khan, P. Kyberd, D. Leslie, I.D. Reid, L. Teodorescu

Boston University, Boston, USA
T. Bose, A. Clough, A. Heister, J. St. John, P. Lawson, D. Lazic, J. Rohlf, L. Sulak

Brown University, Providence, USA
J. Andrea, A. Avetisyan, S. Bhattacharya, J.P. Chou, D. Cutts, S. Esen, U. Heintz, S. Jabeen, G. Kukartsev, G. Landsberg, M. Narain, D. Nguyen, T. Speer, K.V. Tsang

University of California, Davis, Davis, USA
M.A. Borgia, R. Breedon, M. Calderon De La Barca Sanchez, D. Cebra, M. Chertok, J. Conway, P.T. Cox, J. Dolen, R. Erbacher, E. Friis, W. Ko, A. Kopecky, R. Lander, H. Liu, S. Maruyama, T. Miceli, M. Nikolic, D. Pellett, J. Robles, T. Schwarz, M. Searle, J. Smith, M. Squires, M. Tripathi, R. Vasquez Sierra, C. Veelken

University of California, Los Angeles, Los Angeles, USA
V. Andreev, K. Arisaka, D. Cline, R. Cousins, A. Deisher, S. Erhan[1], C. Farrell, M. Felcini, J. Hauser, M. Ignatenko, C. Jarvis, C. Plager, G. Rakness, P. Schlein[†], J. Tucker, V. Valuev, R. Wallny

University of California, Riverside, Riverside, USA
J. Babb, R. Clare, J. Ellison, J.W. Gary, G. Hanson, G.Y. Jeng, S.C. Kao, F. Liu, H. Liu, A. Luthra, H. Nguyen, G. Pasztor[33], A. Satpathy, B.C. Shen[†], R. Stringer, J. Sturdy, S. Sumowidagdo, R. Wilken, S. Wimpenny

University of California, San Diego, La Jolla, USA
W. Andrews, J.G. Branson, E. Dusinberre, D. Evans, F. Golf, A. Holzner, R. Kelley, M. Lebourgeois, J. Letts, B. Mangano, J. Muelmenstaedt, S. Padhi, C. Palmer, G. Petrucciani, H. Pi, M. Pieri, R. Ranieri, M. Sani, V. Sharma[1], S. Simon, Y. Tu, A. Vartak, F. Würthwein, A. Yagil

University of California, Santa Barbara, Santa Barbara, USA
D. Barge, M. Blume, C. Campagnari, M. D'Alfonso, T. Danielson, J. Garberson, J. Incandela, C. Justus, P. Kalavase, S.A. Koay, D. Kovalskyi, V. Krutelyov, J. Lamb, S. Lowette, V. Pavlunin, F. Rebassoo, J. Ribnik, J. Richman, R. Rossin, D. Stuart, W. To, J.R. Vlimant, M. Witherell

California Institute of Technology, Pasadena, USA
A. Bornheim, J. Bunn, M. Gataullin, D. Kcira, V. Litvine, Y. Ma, H.B. Newman, C. Rogan, K. Shin, V. Timciuc, J. Veverka, R. Wilkinson, Y. Yang, R.Y. Zhu

Carnegie Mellon University, Pittsburgh, USA
B. Akgun, R. Carroll, T. Ferguson, D.W. Jang, S.Y. Jun, M. Paulini, J. Russ, N. Terentyev, H. Vogel, I. Vorobiev

University of Colorado at Boulder, Boulder, USA
J.P. Cumalat, M.E. Dinardo, B.R. Drell, W.T. Ford, B. Heyburn, E. Luiggi Lopez, U. Nauenberg, J.G. Smith, K. Stenson, K.A. Ulmer, S.R. Wagner, S.L. Zang

Cornell University, Ithaca, USA
L. Agostino, J. Alexander, F. Blekman, A. Chatterjee, S. Das, N. Eggert, L.J. Fields, L.K. Gibbons, B. Heltsley, W. Hopkins, A. Khukhunaishvili, B. Kreis, V. Kuznetsov, G. Nicolas Kaufman, J.R. Patterson, D. Puigh, D. Riley, A. Ryd, X. Shi, W. Sun, W.D. Teo, J. Thom, J. Thompson, J. Vaughan, Y. Weng, P. Wittich

Fairfield University, Fairfield, USA
A. Biselli, G. Cirino, D. Winn

Fermi National Accelerator Laboratory, Batavia, USA
S. Abdullin, M. Albrow, J. Anderson, G. Apollinari, M. Atac, J.A. Bakken, S. Banerjee, L.A.T. Bauerdick, A. Beretvas, J. Berryhill, P.C. Bhat, I. Bloch, F. Borcherding, K. Burkett, J.N. Butler, V. Chetluru, H.W.K. Cheung, F. Chlebana, S. Cihangir, M. Demarteau, D.P. Eartly, V.D. Elvira, I. Fisk, J. Freeman, Y. Gao, E. Gottschalk, D. Green, O. Gutsche, A. Hahn, J. Hanlon, R.M. Harris, E. James, H. Jensen, M. Johnson, U. Joshi, R. Khatiwada, B. Kilminster, B. Klima, K. Kousouris, S. Kunori, S. Kwan, P. Limon, R. Lipton, J. Lykken, K. Maeshima, J.M. Marraffino, D. Mason, P. McBride, T. McCauley, T. Miao, K. Mishra, S. Mrenna, Y. Musienko[34], C. Newman-Holmes, V. O'Dell, S. Popescu, R. Pordes, O. Prokofyev, N. Saoulidou, E. Sexton-Kennedy, S. Sharma, R.P. Smith[†], A. Soha, W.J. Spalding, L. Spiegel, P. Tan, L. Taylor, S. Tkaczyk, L. Uplegger, E.W. Vaandering, R. Vidal, J. Whitmore, W. Wu, F. Yumiceva, J.C. Yun

University of Florida, Gainesville, USA
D. Acosta, P. Avery, D. Bourilkov, M. Chen, G.P. Di Giovanni, D. Dobur, A. Drozdetskiy, R.D. Field, Y. Fu, I.K. Furic, J. Gartner, B. Kim, S. Klimenko, J. Konigsberg, A. Korytov, K. Kotov, A. Kropivnitskaya, T. Kypreos, K. Matchev, G. Mitselmakher, Y. Pakhotin, J. Piedra Gomez, C. Prescott, R. Remington, M. Schmitt, B. Scurlock, P. Sellers, D. Wang, J. Yelton, M. Zakaria

Florida International University, Miami, USA
C. Ceron, V. Gaultney, L. Kramer, L.M. Lebolo, S. Linn, P. Markowitz, G. Martinez, D. Mesa, J.L. Rodriguez

Florida State University, Tallahassee, USA
T. Adams, A. Askew, J. Chen, B. Diamond, S.V. Gleyzer, J. Haas, S. Hagopian, V. Hagopian, M. Jenkins, K.F. Johnson, H. Prosper, S. Sekmen, V. Veeraraghavan

Florida Institute of Technology, Melbourne, USA
M.M. Baarmand, S. Guragain, M. Hohlmann, H. Kalakhety, H. Mermerkaya, R. Ralich, I. Vodopiyanov

University of Illinois at Chicago (UIC), Chicago, USA
M.R. Adams, I.M. Anghel, L. Apanasevich, V.E. Bazterra, R.R. Betts, J. Callner, R. Cavanaugh, C. Dragoiu, E.J. Garcia-Solis, C.E. Gerber, D.J. Hofman, S. Khalatian, F. Lacroix, E. Shabalina, A. Smoron, D. Strom, N. Varelas

The University of Iowa, Iowa City, USA
U. Akgun, E.A. Albayrak, B. Bilki, K. Cankocak[35], W. Clarida, F. Duru, C.K. Lae, E. McCliment, J.-P. Merlo, A. Mestvirishvili, A. Moeller, J. Nachtman, C.R. Newsom, E. Norbeck, J. Olson, Y. Onel, F. Ozok, S. Sen, J. Wetzel, T. Yetkin, K. Yi

Johns Hopkins University, Baltimore, USA
B.A. Barnett, B. Blumenfeld, A. Bonato, C. Eskew, D. Fehling, G. Giurgiu, A.V. Gritsan, Z.J. Guo, G. Hu, P. Maksimovic, S. Rappoccio, M. Swartz, N.V. Tran, A. Whitbeck

The University of Kansas, Lawrence, USA
P. Baringer, A. Bean, G. Benelli, O. Grachov, M. Murray, V. Radicci, S. Sanders, J.S. Wood, V. Zhukova

Kansas State University, Manhattan, USA
D. Bandurin, T. Bolton, I. Chakaberia, A. Ivanov, K. Kaadze, Y. Maravin, S. Shrestha, I. Svintradze, Z. Wan

Lawrence Livermore National Laboratory, Livermore, USA
J. Gronberg, D. Lange, D. Wright

University of Maryland, College Park, USA
D. Baden, M. Boutemeur, S.C. Eno, D. Ferencek, N.J. Hadley, R.G. Kellogg, M. Kirn, A.C. Mignerey, K. Rossato, P. Rumerio, F. Santanastasio, A. Skuja, J. Temple, M.B. Tonjes, S.C. Tonwar, E. Twedt

Massachusetts Institute of Technology, Cambridge, USA
B. Alver, G. Bauer, J. Bendavid, W. Busza, E. Butz, I.A. Cali, M. Chan, D. D'Enterria, P. Everaerts, G. Gomez Ceballos, M. Goncharov, K.A. Hahn, P. Harris, Y. Kim, M. Klute, Y.-J. Lee, W. Li, C. Loizides, P.D. Luckey, T. Ma, S. Nahn, C. Paus, C. Roland, G. Roland, M. Rudolph, G.S.F. Stephans, K. Sumorok, K. Sung, E.A. Wenger, B. Wyslouch, S. Xie, Y. Yilmaz, A.S. Yoon, M. Zanetti

University of Minnesota, Minneapolis, USA
P. Cole, S.I. Cooper, P. Cushman, B. Dahmes, A. De Benedetti, P.R. Dudero, G. Franzoni, J. Haupt, K. Klapoetke, Y. Kubota, J. Mans, V. Rekovic, R. Rusack, M. Sasseville, A. Singovsky

University of Mississippi, University, USA
L.M. Cremaldi, R. Godang, R. Kroeger, L. Perera, R. Rahmat, D.A. Sanders, P. Sonnek, D. Summers

University of Nebraska-Lincoln, Lincoln, USA
K. Bloom, S. Bose, J. Butt, D.R. Claes, A. Dominguez, M. Eads, J. Keller, T. Kelly, I. Kravchenko, J. Lazo-Flores, C. Lundstedt, H. Malbouisson, S. Malik, G.R. Snow

State University of New York at Buffalo, Buffalo, USA
U. Baur, I. Iashvili, A. Kharchilava, A. Kumar, K. Smith, M. Strang, J. Zennamo

Northeastern University, Boston, USA
G. Alverson, E. Barberis, D. Baumgartel, O. Boeriu, S. Reucroft, J. Swain, D. Wood, J. Zhang

Northwestern University, Evanston, USA
A. Anastassov, A. Kubik, R.A. Ofierzynski, A. Pozdnyakov, M. Schmitt, S. Stoynev, M. Velasco, S. Won

University of Notre Dame, Notre Dame, USA
L. Antonelli, D. Berry, M. Hildreth, C. Jessop, D.J. Karmgard, J. Kolb, T. Kolberg, K. Lannon, S. Lynch, N. Marinelli, D.M. Morse, R. Ruchti, J. Slaunwhite, N. Valls, J. Warchol, M. Wayne, J. Ziegler

The Ohio State University, Columbus, USA
B. Bylsma, L.S. Durkin, J. Gu, P. Killewald, T.Y. Ling, G. Williams

Princeton University, Princeton, USA
N. Adam, E. Berry, P. Elmer, D. Gerbaudo, V. Halyo, A. Hunt, J. Jones, E. Laird, D. Lopes Pegna, D. Marlow, T. Medvedeva, M. Mooney, J. Olsen, P. Piroué, D. Stickland, C. Tully, J.S. Werner, A. Zuranski

University of Puerto Rico, Mayaguez, USA
J.G. Acosta, X.T. Huang, A. Lopez, H. Mendez, S. Oliveros, J.E. Ramirez Vargas, A. Zatzerklyaniy

Purdue University, West Lafayette, USA
E. Alagoz, V.E. Barnes, G. Bolla, L. Borrello, D. Bortoletto, A. Everett, A.F. Garfinkel, Z. Gecse, L. Gutay, M. Jones, O. Koybasi, A.T. Laasanen, N. Leonardo, C. Liu, V. Maroussov, P. Merkel, D.H. Miller, N. Neumeister, K. Potamianos, I. Shipsey, D. Silvers, H.D. Yoo, J. Zablocki, Y. Zheng

Purdue University Calumet, Hammond, USA
P. Jindal, N. Parashar

Rice University, Houston, USA
V. Cuplov, K.M. Ecklund, F.J.M. Geurts, J.H. Liu, J. Morales, B.P. Padley, R. Redjimi, J. Roberts

University of Rochester, Rochester, USA
B. Betchart, A. Bodek, Y.S. Chung, P. de Barbaro, R. Demina, H. Flacher, A. Garcia-Bellido, Y. Gotra, J. Han, A. Harel, D.C. Miner, D. Orbaker, G. Petrillo, D. Vishnevskiy, M. Zielinski

The Rockefeller University, New York, USA
A. Bhatti, L. Demortier, K. Goulianos, K. Hatakeyama, G. Lungu, C. Mesropian, M. Yan

Rutgers, the State University of New Jersey, Piscataway, USA
O. Atramentov, Y. Gershtein, R. Gray, E. Halkiadakis, D. Hidas, D. Hits, A. Lath, K. Rose, S. Schnetzer, S. Somalwar, R. Stone, S. Thomas

University of Tennessee, Knoxville, USA
G. Cerizza, M. Hollingsworth, S. Spanier, Z.C. Yang, A. York

Texas A&M University, College Station, USA
J. Asaadi, R. Eusebi, J. Gilmore, A. Gurrola, T. Kamon, V. Khotilovich, R. Montalvo, C.N. Nguyen, J. Pivarski, A. Safonov, S. Sengupta, D. Toback, M. Weinberger

Texas Tech University, Lubbock, USA
N. Akchurin, C. Bardak, J. Damgov, C. Jeong, K. Kovitanggoon, S.W. Lee, P. Mane, Y. Roh, A. Sill, I. Volobouev, R. Wigmans, E. Yazgan

Vanderbilt University, Nashville, USA
E. Appelt, E. Brownson, D. Engh, C. Florez, W. Gabella, W. Johns, P. Kurt, C. Maguire, A. Melo, P. Sheldon, J. Velkovska

University of Virginia, Charlottesville, USA
M.W. Arenton, M. Balazs, M. Buehler, S. Conetti, B. Cox, R. Hirosky, A. Ledovskoy, C. Neu, R. Yohay

Wayne State University, Detroit, USA
S. Gollapinni, K. Gunthoti, R. Harr, P.E. Karchin, M. Mattson, C. Milstène, A. Sakharov

University of Wisconsin, Madison, USA
M. Anderson, M. Bachtis, J.N. Bellinger, D. Carlsmith, S. Dasu, S. Dutta, J. Efron, L. Gray, K.S. Grogg, M. Grothe, M. Herndon, P. Klabbers, J. Klukas, A. Lanaro, C. Lazaridis, J. Leonard, D. Lomidze, R. Loveless, A. Mohapatra, G. Polese, D. Reeder, A. Savin, W.H. Smith, J. Swanson, M. Weinberg

†: Deceased
1: Also at CERN, European Organization for Nuclear Research, Geneva, Switzerland
2: Also at Universidade Federal do ABC, Santo Andre, Brazil
3: Also at Laboratoire Leprince-Ringuet, Ecole Polytechnique, IN2P3-CNRS, Palaiseau, France
4: Also at Fayoum University, El-Fayoum, Egypt
5: Also at Soltan Institute for Nuclear Studies, Warsaw, Poland
6: Also at Université de Haute-Alsace, Mulhouse, France
7: Also at Moscow State University, Moscow, Russia
8: Also at Institute of Nuclear Research ATOMKI, Debrecen, Hungary
9: Also at Eötvös Loránd University, Budapest, Hungary
10: Also at University of California, San Diego, La Jolla, USA
11: Also at Tata Institute of Fundamental Research - HECR, Mumbai, India
12: Also at University of Visva-Bharati, Santiniketan, India
13: Also at Facolta' Ingegneria Università di Roma "La Sapienza", Roma, Italy
14: Also at Università della Basilicata, Potenza, Italy
15: Also at Laboratori Nazionali di Legnaro dell' INFN, Legnaro, Italy
16: Also at California Institute of Technology, Pasadena, USA
17: Also at Faculty of Physics of University of Belgrade, Belgrade, Serbia
18: Also at Scuola Normale e Sezione dell' INFN, Pisa, Italy
19: Also at INFN Sezione di Roma; Università di Roma "La Sapienza", Roma, Italy
20: Also at University of Athens, Athens, Greece
21: Also at The University of Kansas, Lawrence, USA
22: Also at Institute for Theoretical and Experimental Physics, Moscow, Russia
23: Also at Paul Scherrer Institut, Villigen, Switzerland
24: Also at Vinca Institute of Nuclear Sciences, Belgrade, Serbia
25: Also at Adiyaman University, Adiyaman, Turkey
26: Also at Mersin University, Mersin, Turkey

27: Also at Izmir Institute of Technology, Izmir, Turkey
28: Also at Kafkas University, Kars, Turkey
29: Also at Suleyman Demirel University, Isparta, Turkey
30: Also at Ege University, Izmir, Turkey
31: Also at Rutherford Appleton Laboratory, Didcot, United Kingdom
32: Also at INFN Sezione di Perugia; Università di Perugia, Perugia, Italy
33: Also at KFKI Research Institute for Particle and Nuclear Physics, Budapest, Hungary
34: Also at Institute for Nuclear Research, Moscow, Russia
35: Also at Istanbul Technical University, Istanbul, Turkey